

**Molecular and Cellular Mechanisms of Increased
Angiogenesis in Multiple Myeloma:
A Role for CXCL12**

Sally K. Martin

Myeloma Research Group
Bone and Cancer Research Laboratory,
Division of Haematology,
Hanson Institute
Institute of Medical and Veterinary Science

&

Department of Medicine,
Faculty of Health Sciences
University of Adelaide



A thesis submitted to the University of Adelaide
for the degree of Doctor of Philosophy
December 2008

Chapter 5:

**THE ROLE OF CXCL12 AND
HYPOXIA IN ANGIOGENESIS
*IN VIVO***

5.1 Introduction

In vitro angiogenesis assays provide important insights into cellular behaviour and are commonly used to examine specific EC processes such as migration, proliferation and tube formation. However, a more complete appraisal of an angiogenic response requires *in vivo* examination. Many different *in vivo* systems have been developed to assess angiogenesis, and each has its own unique benefits and limitations in terms of invasiveness, reproducibility, experimental ease, cost and time required.

In general, *in vivo* angiogenesis assays can be divided into three main categories: microcirculatory animal preparations, vascularisation into biocompatible scaffolds, and examination of excised tissues. (1) “*Microcirculatory animal preparations*” involve the implantation of cells, tissues or chemicals into transparent chambers (eg. ear chamber, dorsal skinfold chamber, or cheek pouch window), exterior tissue preparations (eg. chick embryo chorioallantoic membrane [CAM] assay), or *in situ* preparations (eg. corneal pocket implant or iris implant). In these assays, angiogenesis is able to be continuously monitored through transparent windows using light microscopy^{474,475}. (2) “*Vascularisation into a biocompatible scaffold*” involves the implantation of cells or factors in a supportive scaffold, and angiogenesis is measured at a single time point by enumerating the number of blood vessels induced by the implanted cells or factors following the removal of the implant from the host. These assays require relatively simple surgical procedures and are often used for high-throughput compound screening⁴⁷⁴. (3) “*Examination of excised tissues*” involves the assessment of vascularity in tissue samples removed from living hosts at a single time point. This approach is generally used to assess the effect of systemically administered drugs on angiogenesis, however due to significant intra- and inter-tissue variability, large numbers of samples are required to obtain definitive results⁴⁷⁴.

Each assay system has its own unique strengths and weaknesses, and investigators must choose the approach which best meets their specific requirements. For example, where a study involves large scale screening of putative angiogenic or angiostatic agents, cost-effective and technically simple assays such as the chick embryo CAM assay are most appropriate. Alternatively, where a study involves detailed examination of the structural and functional characteristics of *de novo* neovascularisation, assays such as the rabbit corneal micropocket are most appropriate because the cornea is completely avascular and allows experimentally-induced angiogenesis to be examined without being obscured by

background vasculature⁴⁷⁶. However, in many *in vivo* angiogenesis assays newly-formed blood vessels are exposed to oxygen, which makes them unsuitable for investigating tumour angiogenesis because hypoxia is a major driving force in tumour angiogenesis. In this instance, matrix implant and hollow fibre assays are most appropriate because they are able to replicate the hypoxic tumour microenvironment⁴⁷⁵.

As CXCL12 is highly conserved between species (differing by only one amino acid between mouse and human)⁴⁷⁷, exogenous human CXCL12 is able to bind and activate murine EC-expressed CXCR4. The ability of CXCL12 to induce *in vivo* angiogenesis has been shown using several different approaches, including the direct subcutaneous injection of rhCXCL12¹⁰, subcutaneous injection of rhCXCL12 in a Matrigel matrix²⁵⁶⁻²⁵⁸, and injection of rhCXCL12 into the rabbit corneal micropocket¹⁴.

The contribution of CXCL12 to pathological tumour angiogenesis remains controversial, however several studies have shown that CXCL12 is an important mediator of this process. The administration of CXCR4 antagonists to mice harbouring subcutaneously implanted gastrointestinal tumour cells⁴⁷⁸, prostate cancer cells²²⁶ and breast cancer cells^{226,479} significantly reduces tumour growth through the suppression of tumour angiogenesis. Furthermore, using a co-implantation xenograft model of breast carcinoma, studies by Orimo *et al*²⁴² have shown that carcinoma-associated fibroblasts and breast cancer cells synergistically enhance tumour angiogenesis and administration of a CXCL12 neutralising antibody significantly reduced this effect. Kollmar and colleagues⁴⁸⁰ have also shown that the addition of exogenous CXCL12 to colorectal tumour cells in the dorsal skinfold chamber assay accelerates blood vessel formation.

This chapter outlines *in vivo* experiments conducted to investigate the role of MM-derived CXCL12 in mediating angiogenesis *in vivo* and the contribution of the HIF transcription factors to this process.

5.2 Results

5.2.1 Development and characterisation of a murine model to assess *in vivo* angiogenesis.

5.2.1.1 *Model 1: Intratibial injection of MM PCs and immunohistochemical assessment of angiogenesis.*

Although numerous animal models which replicate key features of human MM disease have been described⁴⁸¹⁻⁴⁸⁴, we chose to establish a localised model of MM in which MM PCs are directly injected into the tibial cavity of immunocompromised nude mice (Figure 5.1A). In preliminary studies, LP-1 cells engineered to express the SFG_{NES}-TGL luciferase reporter construct (abbreviated to LP-1-SFG), or an equivalent volume of PBS, were injected into mice (Figure 5.1A) and tumour growth was monitored weekly for five weeks using *in vivo* bioluminescence imaging following intraperitoneal administration of D-luciferin substrate (Figure 5.1B). Pseudocolour bioluminescence images were overlaid on greyscale images of each mouse to determine the signal intensity arising from the injected tumour cells. Over time, an increase in the diameter and intensity of the luminescence signal emitted from implanted MM PCs was observed, proportional to the increasing tumour burden (Figure 5.1B).

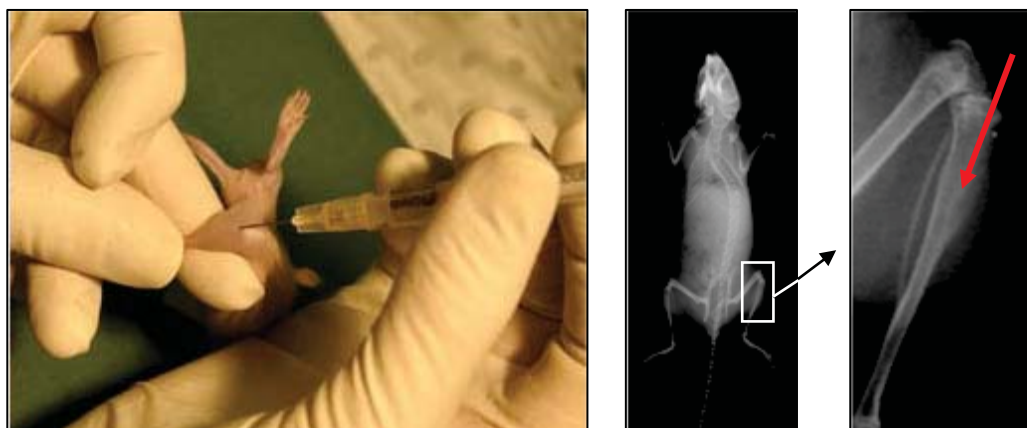
After five weeks, the mice were humanely killed and the hind legs dissected, fixed, decalcified and embedded in paraffin. To investigate whether BM MVD, a surrogate marker of angiogenesis, was elevated in mice receiving LP-1-SFG cells compared to the PBS control, sections of paraffin-embedded hind leg specimens were stained with an EC-reactive anti-CD31 antibody. Unfortunately, repeated attempts at assessing BM MVD in these specimens were unsuccessful and an alternative approach was sought.

5.2.1.2 *Model 2: Subcutaneous injection of MM PCs in Matrigel Matrix and immunohistochemical assessment of angiogenesis.*

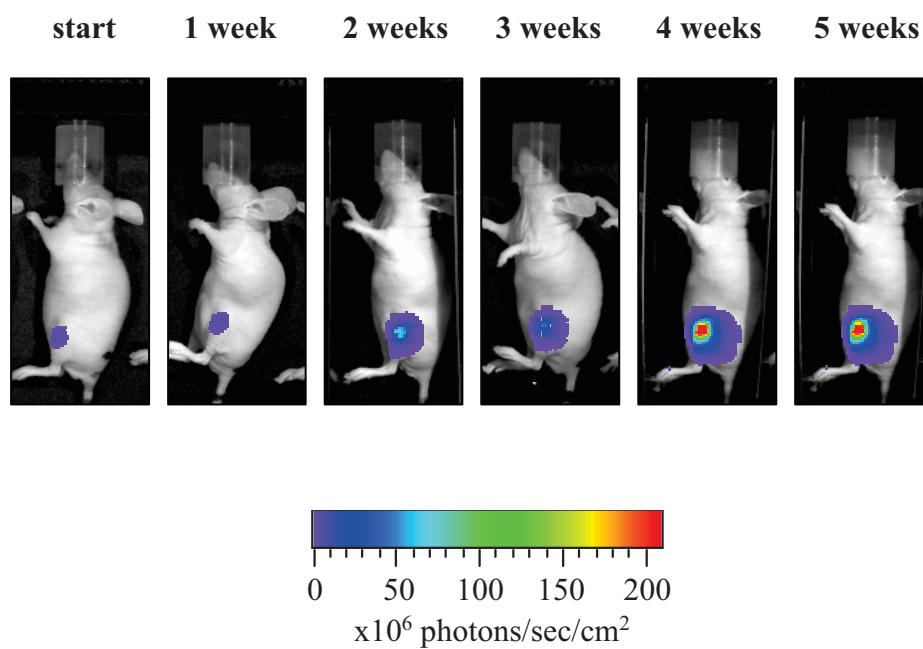
To assess whether angiogenesis could be measured in subcutaneously implanted MM PCs, a pilot study was performed in which LP-1-SFG cells were mixed in liquid Matrigel and subcutaneously implanted into immunocompromised nude mice. Preliminary titration experiments were performed to establish the optimal number of MM PCs required to stimulate *de novo* vessel formation in this model. In these studies, Matrigel implants containing three different cell concentrations were examined: 1×10^6 , 5×10^6 , and 1×10^7 cells/ implant, with each mouse receiving two identical implants.

Figure 5.1. Intratibial Injection of MM PCs. (A) LP-1 MM PCs transduced with the SFG_{NES}-TGL luciferase reporter construct were injected into the tibial cavity of 4-week old immunocompromised mice (1×10^6 cells/ injection). (B) Using *in vivo* bioluminescence imaging, tumour growth was assessed at weekly intervals for five weeks following the administration of D-luciferin substrate. At each time point, pseudocolour bioluminescence images were recorded and overlaid onto grayscale photographs, and the bioluminescence signal intensity measured as photons/second/cm². These images are representative of an animal cohort containing at least five animals.

A



B



Tumour growth was monitored weekly for five weeks using *in vivo* bioluminescence imaging (Figure 5.2). In the mice which received implants containing 1×10^6 and 5×10^6 cells, a time-dependent increase in bioluminescence signal intensity and diameter was observed. In contrast, a dramatic decrease in bioluminescence was observed immediately following the implantation of 1×10^7 cells, which was followed by a progressive increase in bioluminescence thereafter.

Using Living Image[®] analysis software, the luminescence signal intensity emitted from each implant was measured, and the cumulative data plotted in Figure 5.3. Over the five week period, a progressive increase in bioluminescence signal intensity was observed in mice bearing 1×10^6 cell implants (Figure 5.3A and Figure 5.3B) and 5×10^6 cell implants (Figure 5.3C and Figure 5.3D). In contrast, a marked decrease in bioluminescence signal was observed in some animals receiving 1×10^7 cell implants (Figure 5.3E). A smaller initial decrease in bioluminescence was observed in other 1×10^7 cell implants (Figure 5.3F), which was followed by a progressive increase in signal at all later time points.

After five weeks, the mice were humanely killed and the Matrigel implants excised. To examine whether frozen specimens were more suitable for CD31 immunohistochemistry than paraffin-embedded specimens, half of the Matrigel implants were fixed and embedded in paraffin, and the other half were frozen in OCT freezing compound. Using an EC-reactive anti-CD31 antibody, MVD was assessed in sections of paraffin-embedded and frozen implant specimens to assess whether increasing numbers of LP-1-SFG cells affected the level of angiogenesis. However, due to significant levels of Matrigel resorption *in vivo*, the size of the recovered samples was found to be inadequate for accurate MVD assessment, and an alternative method of assessing angiogenesis was sought. Furthermore, no difference between paraffin-embedded and frozen specimens was observed.

5.2.1.3 Drabkin's assessment of haemoglobin content to measure angiogenesis.

Given the repeated difficulties encountered with assessing angiogenesis by immunohistochemical methods, we examined whether the Drabkin's method of haemoglobin assessment was a suitable alternative approach. Preliminary studies were performed to test the sensitivity of the Drabkin's method using numerous murine tissue samples known to contain variable levels of vascularity. In these studies, tissue samples were harvested, sonicated and the haemoglobin content measured using the Drabkin's

Figure 5.2. Bioluminescence Monitoring of Subcutaneous MM PC Tumour Growth.

LP-1 MM PCs transduced with the SFG_{-NES}-TGL luciferase reporter construct were mixed in liquid Matrigel (1×10^6 , 5×10^6 or 1×10^7 cells/ implant) and injected subcutaneously into immunocompromised mice. Each mouse received two identical implants. The injected Matrigel rapidly formed a solid plug upon gentle heating under a heat lamp. Using *in vivo* bioluminescence imaging, tumour growth was assessed at weekly intervals for five weeks following the administration of D-luciferin substrate. At each time point, pseudocolour bioluminescence images were recorded and overlaid onto grayscale photographs, and the bioluminescence signal intensity measured as photons/second/cm². These images are representative of animal cohorts containing at least three animals.

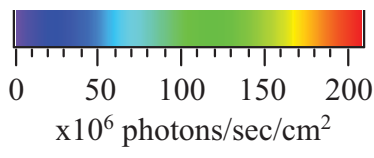
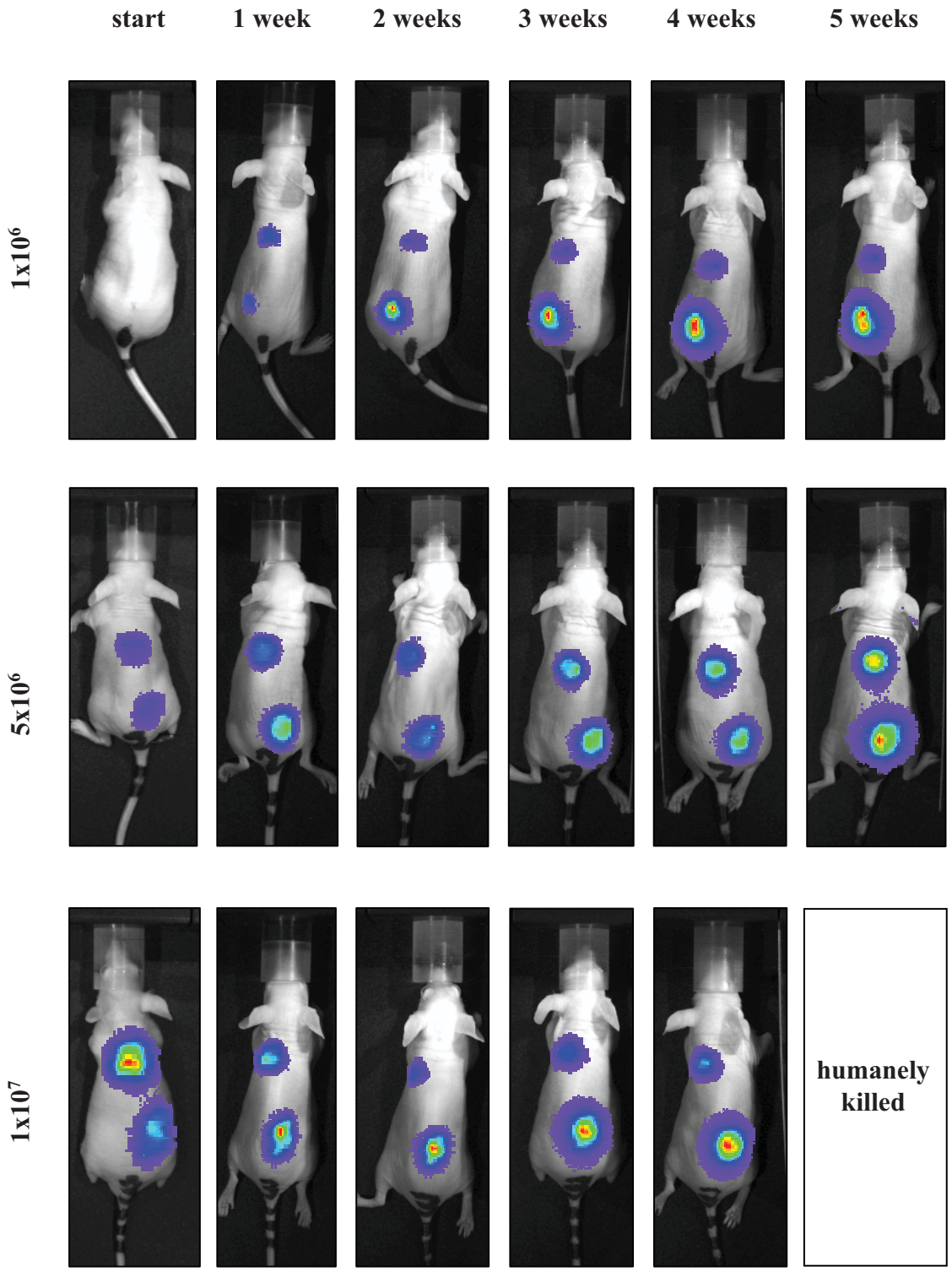
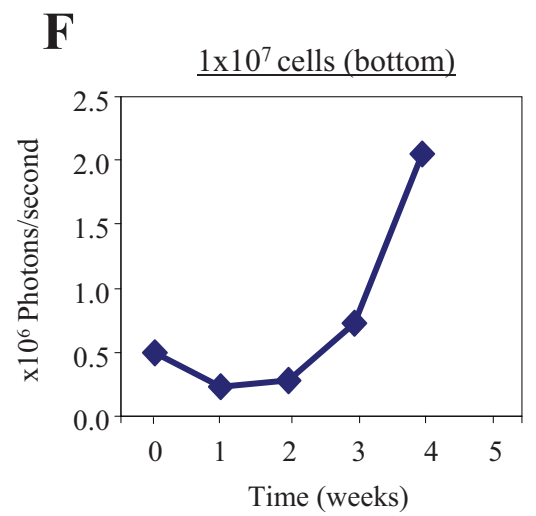
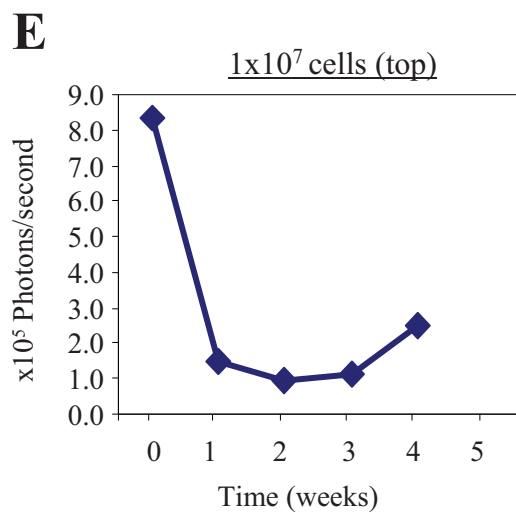
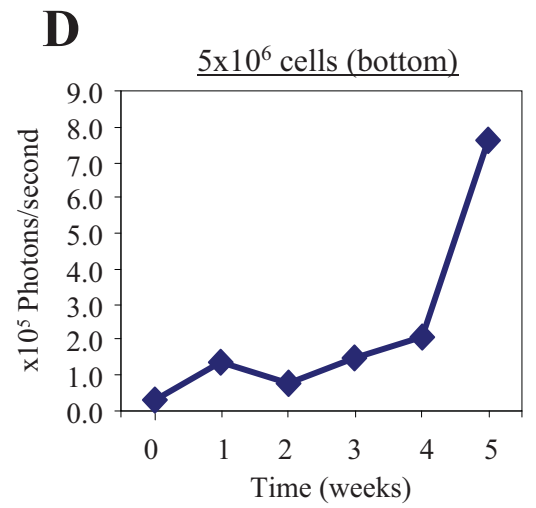
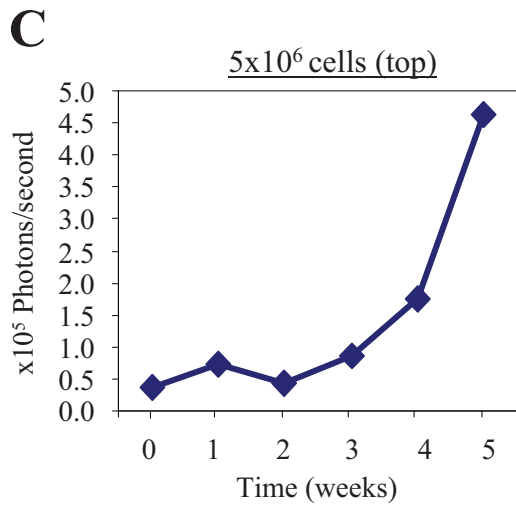
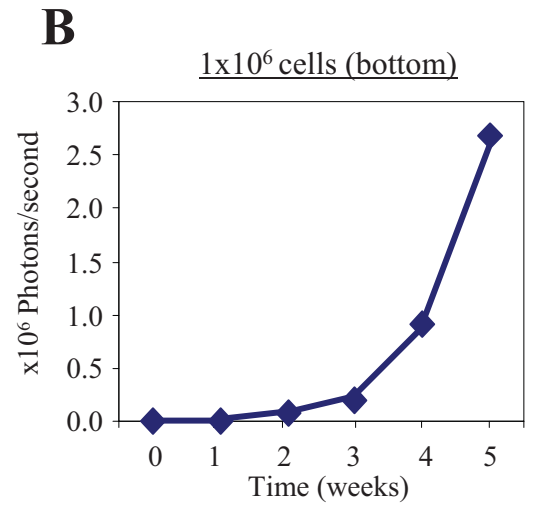
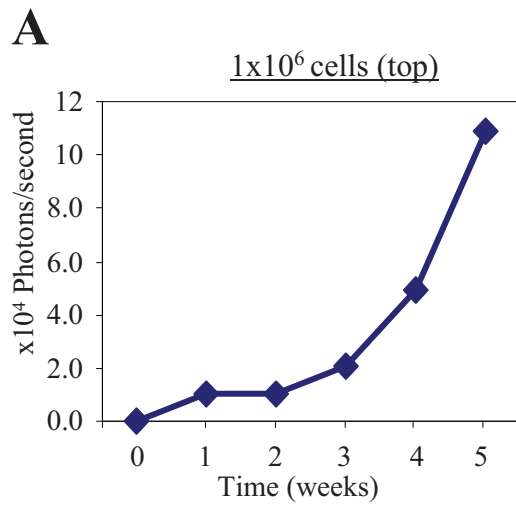


Figure 5.3. Quantitation of Bioluminescence Monitoring of Subcutaneous MM PC Tumour Growth. As illustrated in Figure 5.2, LP-1 MM PCs transduced with the SFG_{-NES}-TGL luciferase reporter construct (1×10^6 , 5×10^6 or 1×10^7 cells/ implant) were injected subcutaneously into immunocompromised mice and tumour growth was monitored over five weeks using *in vivo* bioluminescence imaging. Living Image[®] analysis software was used to quantitate the bioluminescence signal intensities of the cell implants at each of the time points examined. Graphical representation of these data illustrates the cumulative changes in bioluminescence signal intensity in the (A) top 1×10^6 cell implant, (B) bottom 1×10^6 cell implant, (C) top 5×10^6 cell implant, (D) bottom 5×10^6 cell implant, (E) top 1×10^7 cell implant, and (F) bottom 1×10^7 cell implant in representative mice. Data are expressed as luminescent photons per second, and are representative of animal cohorts containing at least three animals.



assay. Haemoglobin concentrations were normalised to the weight of each respective sample, to provide a relative measure of vascularity (Figure 5.4). Haemoglobin was detected in all tissue samples tested, ranging from 0.4mg/mL in a sample of skin/fur to 31mg/mL in a sample of lung tissue (Figure 5.4). On the basis of these findings, the Drabkin's assay was considered to be sufficiently sensitive to assess the vascularity of Matrigel implants.

5.2.1.4 *The final model: Subcutaneous injection of MM PCs in Matrigel and Drabkin's assessment of angiogenesis.*

The studies described thus far were performed to identify and characterise a suitable murine model to investigate the role of CXCL12 in mediating *in vivo* angiogenesis, and the contribution of the HIF transcription factors in this process. The final model arising from these preliminary studies is outlined in Figure 5.5. In this model, transduced LP-1 cells harbouring the SFG_{-NES}-TGL luciferase reporter construct (5×10^6 cells/ implant) were mixed in liquid Matrigel and implanted subcutaneously into the right ventral flank of immunocompromised nude mice. As a negative control, a Matrigel implant containing no cells was implanted into the left ventral flank of each mouse (Figure 5.5A). For experiments in which the role of CXCL12/CXCR4 in mediating *in vivo* angiogenesis was to be examined, Alzet osmotic pumps containing the CXCR4 antagonist, T140, were implanted subcutaneously into the upper dorsum of half of the animals. Tumour growth was monitored weekly for two weeks using *in vivo* bioluminescence imaging (Figure 5.5B), after which the mice were humanely killed and the implants excised and photographed (Figure 5.5C). The implants were weighed and the haemoglobin content of each implant measured using the Drabkin's assay. Drabkin's data were normalised to the weight of the respective sample, to provide a relative measure of vascularity (Figure 5.5D).

5.2.2 The creation and characterisation of CXCL12 over-expression and CXCL12 knockdown in LP-1 cells.

5.2.2.1 *CXCL12 over-expression in LP-1 cells.*

In order to further examine the contribution of MM-derived CXCL12 to tumour angiogenesis, LP-1 cells were engineered to stably over-express CXCL12 via retroviral infection with a bi-cistronic pRUF vector containing a CXCL12 over-expression construct (as described in Section 2.7, Materials and Methods). Transduced cells were subsequently sorted on the basis of GFP expression, with the top 30% of GFP-expressing cells

Figure 5.4. Quantitation of *In Vivo* Angiogenesis Using Drabkin's Assessment of Haemoglobin Content. Tissue samples were taken of numerous murine tissues and the haemoglobin content of these samples determined using the Drabkin's assay. To test the sensitivity of this assay, the tissue samples were taken from sites known to contain variable levels of vascularity. Graphical representation of these data illustrates the haemoglobin content detected in each tissue, normalised to sample weight. Data are expressed as mean \pm standard deviation from replicate samples.

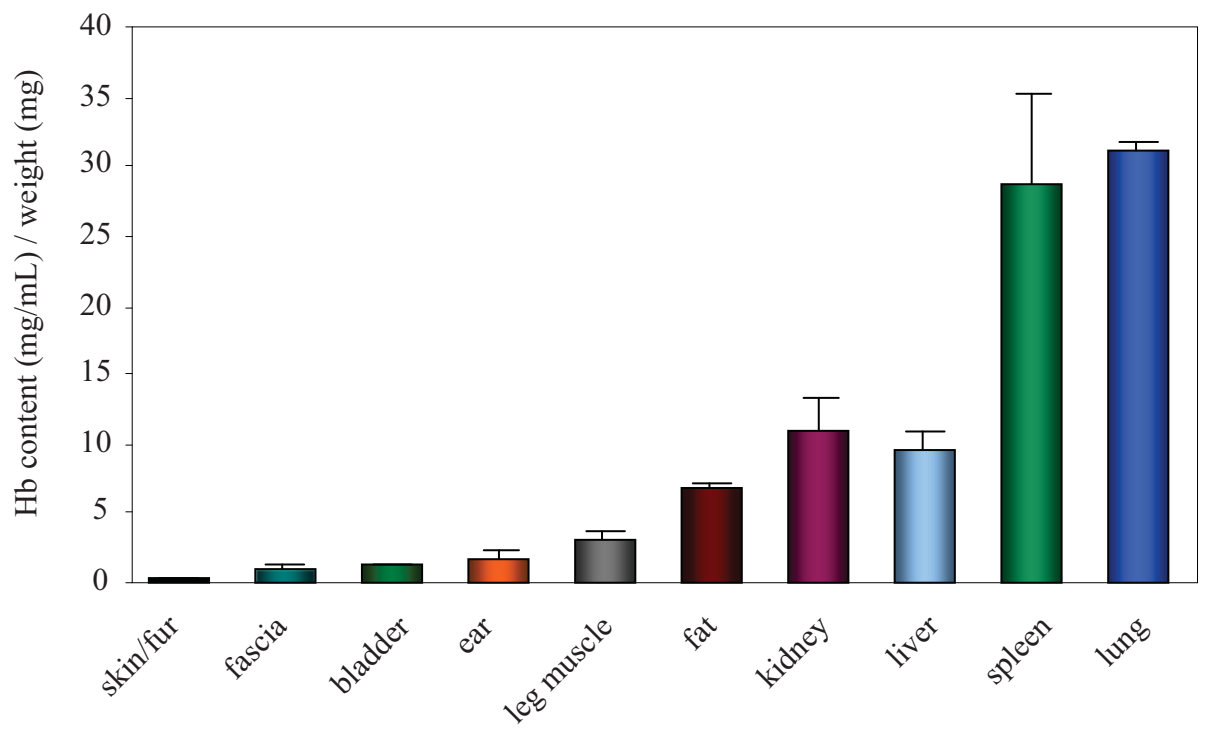
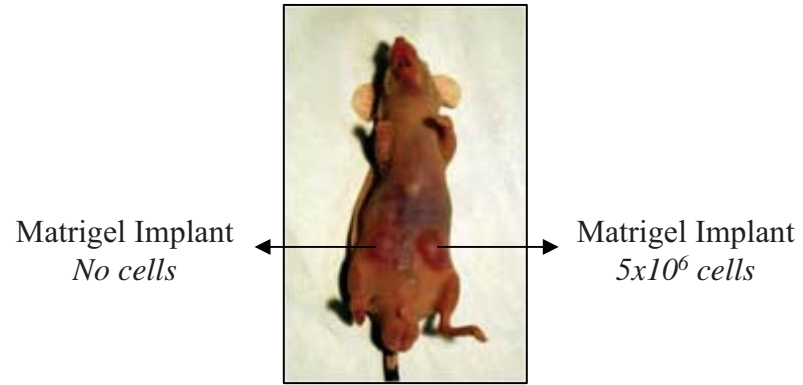
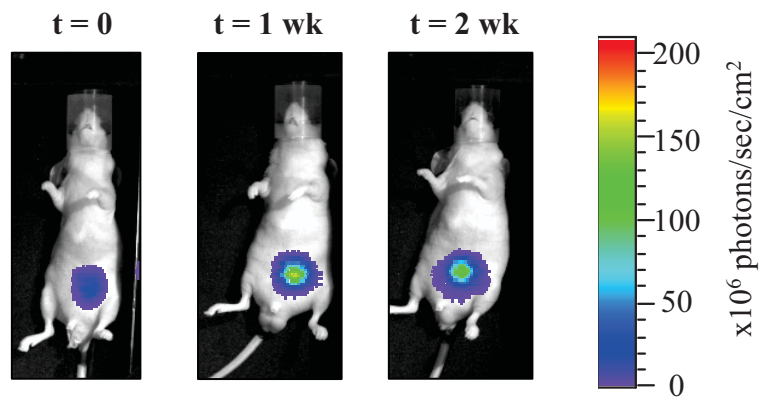
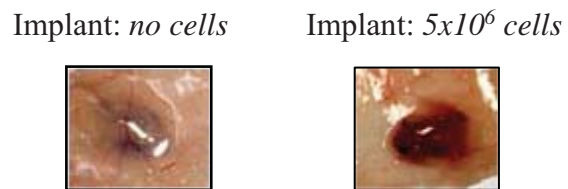
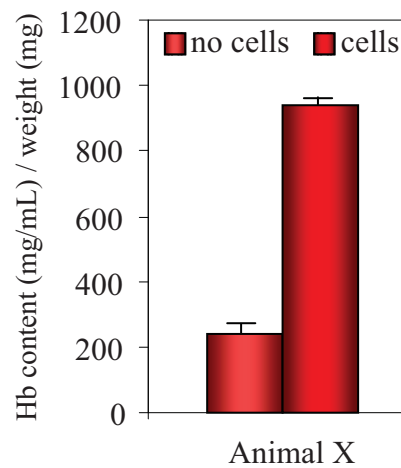


Figure 5.5. Final Characterisation of the *In Vivo* Model of Angiogenesis. (A) 5×10^6 LP-1 MM PCs transduced with the SFG_{-NES}-TGL luciferase reporter construct were mixed in liquid Matrigel and injected subcutaneously into the right ventral flank of immunocompromised mice. As a negative control, a Matrigel implant containing no cells was implanted into the left ventral flank of each mouse. Injected Matrigel implants rapidly formed solid plugs upon gentle heating under a heat lamp. (B) Using *in vivo* bioluminescence imaging, tumour growth was assessed at weekly intervals for two weeks following the administration of D-luciferin substrate. At each time point, pseudocolour bioluminescence images were recorded and overlaid onto grayscale photographs, and the bioluminescence signal intensity measured as photons/second/cm². (C) After two weeks, the mice were humanely killed, and macroscopic photographs taken of each implant. (D) Following careful dissection of the implant from the surrounding tissue, implants were weighed and the haemoglobin content of each implant measured using the Drabkin's assay. Drabkin's data were normalised to the weight of each tissue sample, to give a relative determination of vascularity per milligram of sample. Data are expressed as mean \pm standard deviation from replicate samples.

A**B****C****D**

harbouring the CXCL12 over-expression construct or the pRUF vector control selected (Figure 5.6A).

Using real-time PCR, the relative levels of *CXCL12* mRNA expression were measured in the CXCL12-over-expressing LP-1 cells (abbreviated to LP-1-CXCL12) and compared to the parental LP-1 cell line and the pRUF vector control (abbreviated to LP-1-pRUF). Constitutive over-expression of CXCL12 was confirmed in LP-1-CXCL12 cells, with a 97,740-fold increase in relative *CXCL12* mRNA expression observed compared to the LP-1 and LP-1-pRUF controls (Figure 5.6B, $p < 0.0001$, one-way ANOVA).

In parallel studies, the relative level of CXCL12 protein expression was examined in these cell lines. Following 72 hours of culture, supernatant was collected from the LP-1, LP-1-pRUF and LP-1-CXCL12 cell lines and CXCL12 protein levels measured using an ELISA (Figure 5.6C). Culture supernatants collected from the LP-1 and LP-1-pRUF cell lines contained 30.6 ± 6.0 pg/mL and 31.9 ± 9.1 pg/mL CXCL12, respectively. Importantly, supernatant from LP-1-CXCL12 cells contained 815.8 ± 31.2 pg/mL CXCL12, demonstrating a 27.2-fold increase in CXCL12 protein compared to the LP-1 and LP-1-pRUF cell lines (Figure 5.6C, $p < 0.0001$, one-way ANOVA).

5.2.2.2 *CXCL12 knockdown in LP-1 cells.*

In addition to the over-expression of CXCL12 in LP-1 cells, a stable knockdown of CXCL12 was created using the pFIV lentiviral vector containing a CXCL12 RNAi sequence or the empty pFIV vector alone (as described in Section 2.7, Materials and Methods). Lentivirally-transduced LP-1 cells were subsequently sorted on the basis of GFP expression, with the top 30% of GFP-expressing cells collected for each cell line (Figure 5.7A). In order to obtain a cell line harbouring the greatest knockdown of CXCL12, clonal populations were created from the top 6.3% of sorted CXCL12 RNAi cells using preparative cell sorting and single cell deposition.

To assess the level of CXCL12 knockdown in these RNAi clones and examine whether the CXCL12 knockdown was maintained under hypoxic conditions, cells were cultured under normoxic or hypoxic conditions for 48 hours and levels of *CXCL12* mRNA expression measured using real-time PCR (Figure 5.7B). Under normoxic conditions, a 75% - 95% suppression of *CXCL12* mRNA expression was observed in all of the clones tested

Figure 5.6. The Creation of CXCL12- Over-Expressing LP-1 Cells. (A) LP-1 cells were engineered to stably over-express CXCL12 via retroviral infection, and the top 30% of transduced cells were selected based on the level of GFP expression. (B) Stable over-expression of *CXCL12* mRNA in these sorted cells was assessed using real-time PCR, and the data normalised to the standard housekeeping gene, *β 2-microglobulin*. Graphical representation of these data illustrates relative levels of *CXCL12* mRNA expression in the parental LP-1 cell line, the pRUF vector control and CXCL12-over-expressing cells. To better display the lower levels of *CXCL12* expression in the LP-1 and vector control cell lines, the graph for the CXCL12 over-expressing cells has been truncated and the true value is displayed above it. Data are expressed as the mean \pm standard deviation of replicate samples and are representative of three individual experiments. * $p < 0.0001$, one-way ANOVA. (C) Using a CXCL12-specific ELISA, levels of CXCL12 protein expression were measured in conditioned media collected from LP-1, LP-1-pRUF and LP-1-CXCL12 cells following 72 hours of culture. Graphical representation of these data illustrates the levels of CXCL12 protein detected in each cell supernatant, normalised to total cellular protein concentration. Data are expressed as mean \pm standard deviation from replicate samples of a representative experiment of three. * $p < 0.0001$, one-way ANOVA.

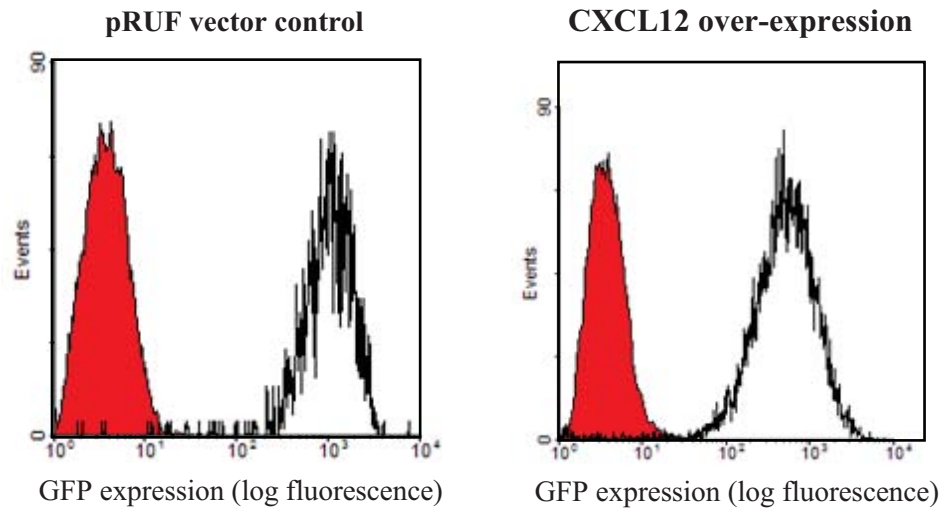
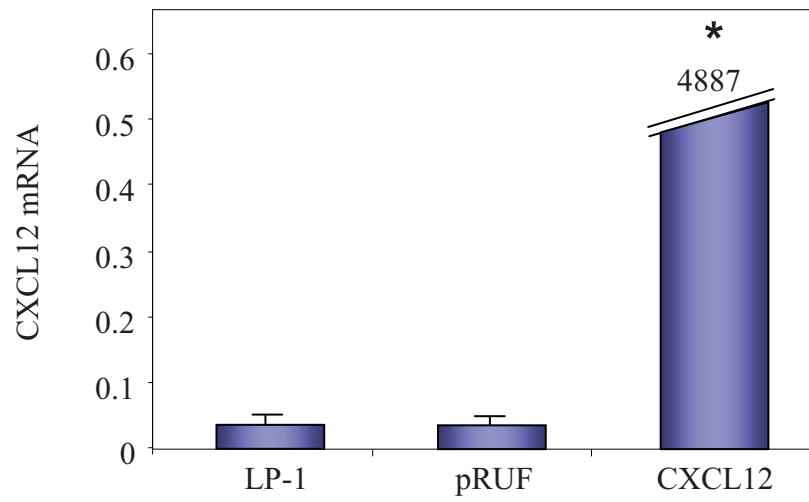
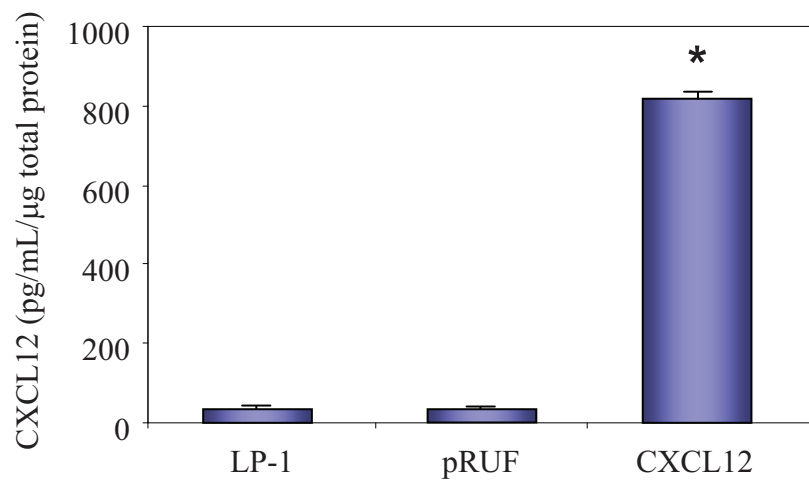
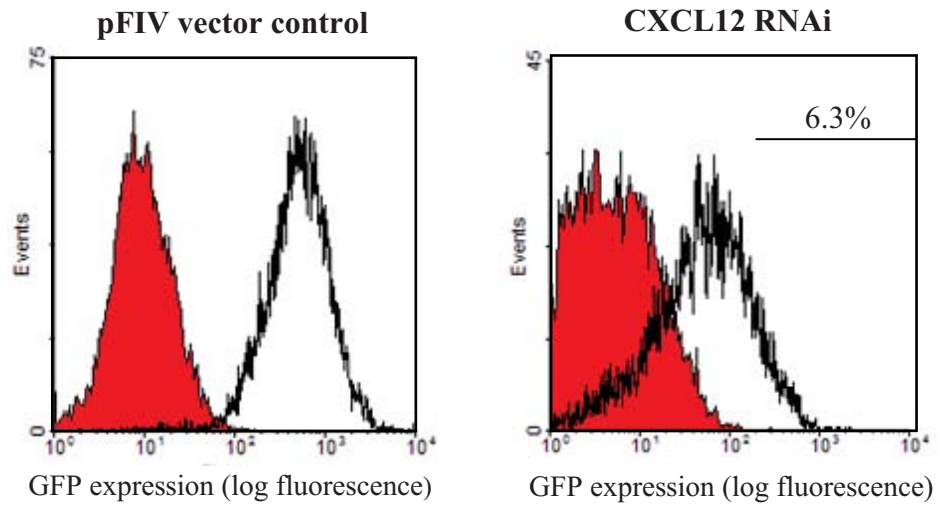
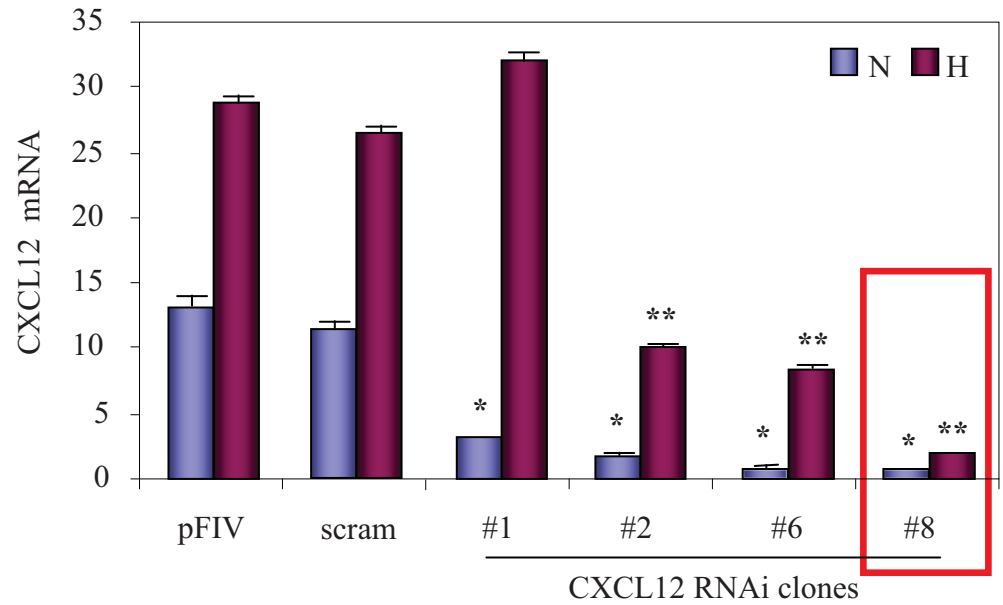
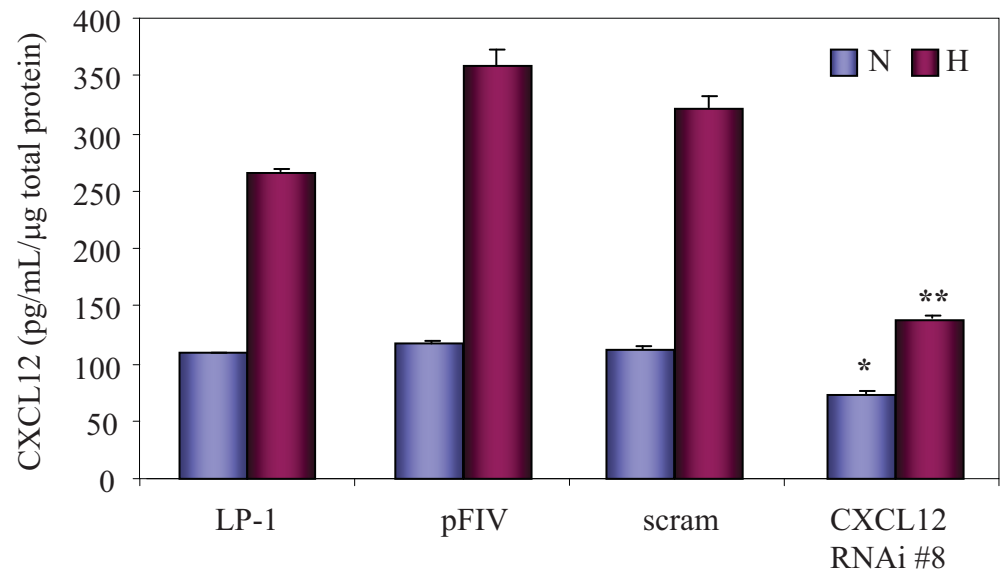
A**B****C**

Figure 5.7. The Creation of CXCL12 Knockdown in LP-1 Cells. (A) RNA interference technology was used to knock down endogenous CXCL12 expression in LP-1 cells, and the top 30% of lentivirally transduced cells were selected based on the level of GFP expression. Single cell clones were then created from the top 6.3% of these sorted GFP-expressing cells. (B) Using real-time PCR, clones were screened for levels of *CXCL12* mRNA expression following culture under normoxic (■) or hypoxic (■) conditions for 48 hours, and data were normalised to the standard housekeeping gene, *β2-microglobulin*. Data are expressed as the mean ± standard deviation of replicate samples and are representative of three individual experiments. *p<0.001 and **p<0.001, one-way ANOVA. (C) Using CXCL12-specific ELISA, levels of CXCL12 protein expression were measured in conditioned media collected from LP-1, LP-1-pFIV and CXCL12 RNAi Clone#8 cells cultured under normoxic (■) or hypoxic (■) conditions for 72 hours. Graphical representation of these data illustrates the levels of CXCL12 protein detected in each cell supernatant, normalised to total cellular protein concentration. Data are expressed as mean ± standard deviation from replicate samples of a representative experiment of three. *p<0.05 and **p<0.001, one-way ANOVA.

A**B****C**

(designated #1, #2, #6 and #8) compared to LP-1-pFIV and LP-1-scramRNAi (Figure 5.7B, $p < 0.001$, one-way ANOVA). In hypoxic conditions, varying degrees of *CXCL12* suppression were observed amongst the RNAi clones, ranging from 0% - 98% knockdown (Figure 5.7B, $p < 0.001$, one-way ANOVA). Under both normoxic and hypoxic culture conditions, “Clone #8” displayed the strongest level of knockdown of *CXCL12* mRNA expression.

To confirm knockdown of *CXCL12* at the protein level, LP-1, LP-1-pFIV, LP-1-scramRNAi and LP-1-*CXCL12* RNAi “Clone #8” cells were cultured under normoxic or hypoxic conditions for 72 hours and levels of *CXCL12* protein in the resultant supernatants measured by ELISA. The culture supernatant collected from LP-1 cells contained 110.7 ± 3.1 pg/mL (normoxia) and 269.4 ± 5.9 pg/mL (hypoxia) *CXCL12* protein, the supernatant from LP-1-FIV cells contained 118.7 ± 3.2 pg/mL (normoxia) and 361.7 ± 10.1 pg/mL (hypoxia) *CXCL12* protein, and the supernatant from LP-1-scramRNAi cells contained 109.7 ± 2.5 pg/mL (normoxia) and 321.0 ± 15.3 pg/mL (hypoxia) *CXCL12* protein. Importantly, culture supernatant from LP-1-*CXCL12* RNAi “Clone #8” cells contained 75.6 ± 4.8 pg/mL (normoxia) and 138.5 ± 4.3 pg/mL (hypoxia) *CXCL12* protein, representing a 37% and 61% reduction respectively, compared to the LP-1-pFIV vector control (Figure 5.7C, $*p < 0.05$ and $**p < 0.001$, one-way ANOVA).

On the basis of these real-time PCR and ELISA data, “Clone #8” was identified as exhibiting the greatest knockdown of *CXCL12* at both the mRNA and protein levels and was used for all subsequent experiments. Hereafter, these cells are referred to as LP-1-*CXCL12*-KD.

5.2.3 Characterisation of all engineered LP-1 cell lines created for this project.

Prior to the implantation of transduced LP-1 cells into mice, it was necessary to characterise all of the over-expression and knockdown cell lines created in this project (in both the preceding and current chapter): LP-1-pRUF, LP-1-*CXCL12*, LP-1-HIF-1 α , LP-1-HIF-2 α , LP-1-pFIV, LP-1-scramRNAi, LP-1-*CXCL12*-KD, LP-1-HIF-1 α -KD, and LP-1-HIF-2 α -KD. As outlined below, levels of *CXCL12* and *CXCR4* protein expression were examined in each of these cell lines, and the rates of cell proliferation compared.



5.2.3.1 *CXCL12 and CXCR4 expression in all engineered LP-1 cell lines.*

Following 72 hours of culture under normoxic or hypoxic conditions, supernatant was collected from each cell line and levels of CXCL12 protein measured using an ELISA (Figure 5.8). CXCL12 protein expression was strongly up-regulated by hypoxia in the LP-1-pRUF, LP-1-pFIV and LP-1-scramRNAi control cell lines. Under normoxic conditions, increased CXCL12 protein levels were detected in the LP-1CXCL12, LP-1-HIF-1 α and LP-1-HIF-2 α cell lines compared to LP-1-pRUF ($p < 0.05$, one-way ANOVA). Under normoxic and hypoxic conditions, a significant reduction in CXCL12 expression was observed in LP-1-CXCL12-KD cells compared to LP-1-pFIV (* $p < 0.05$ and ** $p < 0.05$, one-way ANOVA). While a significant reduction in CXCL12 expression was also observed in both of the HIF knockdown cell lines compared to LP-1-pFIV under hypoxic conditions ($p < 0.05$, one-way ANOVA), this was not evident under normoxic culture conditions.

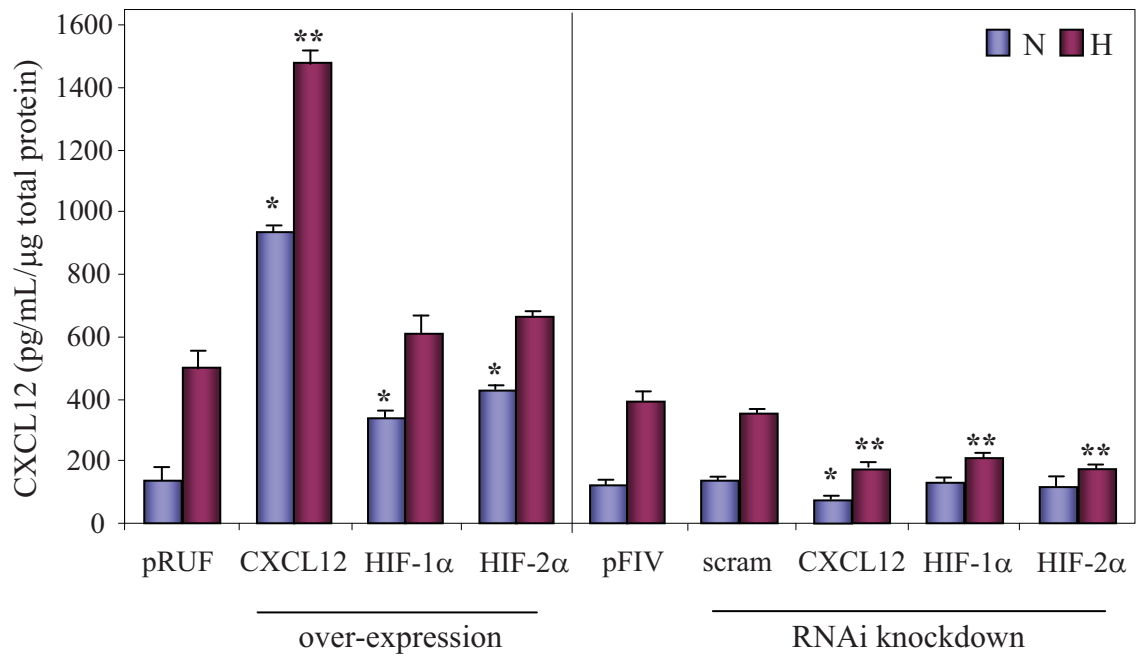
In parallel studies, levels of CXCR4 protein expression were measured in each of the transduced LP-1 cell lines using flow cytometry. With the exception of the LP-1-CXCL12 cell line, strong CXCR4 protein expression was detected in all cell lines: LP-1-pRUF (Figure 5.9A, MFI=6.9), LP-1-HIF-1 α (Figure 5.9C, MFI=9.7), LP-1-HIF-2 α (Figure 5.9D, MFI=4.4), LP-1-pFIV (Figure 5.9E, MFI=10.5), LP-1-scramRNAi (Figure 5.9F, MFI=9.2), LP-1-CXCL12-KD (Figure 5.9G, MFI=9.9), LP-1-HIF-1 α -KD (Figure 5.9H, MFI=6.5) and LP-1-HIF-2 α -KD (Figure 5.9I, MFI=7.8). In contrast, minimal CXCR4 expression was detected in the LP-1-CXCL12 cell line (Figure 5.9B, MFI=0.3), which was attributed to the saturating levels of CXCL12 mediating rapid internalisation and degradation of the CXCR4 receptor¹⁵⁸.

5.2.3.2 *The proliferation rates of all engineered LP-1 cell lines.*

A WST-1 proliferation assay was performed to compare the rates of proliferation between the transduced LP-1 cell lines. Each cell line was seeded at the same density, and the relative numbers of viable cells assessed following 1, 3, 5, and 7 days of culture. No significant difference was observed following 1, 3 and 5 days of culture, however modest differences were found after 7 days (Figure 5.10A, $p = 0.15$, one-way ANOVA). To better display overall rate of cell proliferation over the 7 day period, the data were re-plotted to reflect the fold change in WST-1 absorbance at day 7 compared to day 1 for each cell line

Figure 5.8. CXCL12 Expression in All Transduced LP-1 Cell Lines. Levels of CXCL12 protein expression were measured in conditioned media from each of the transduced LP-1 cell lines created for this project: LP-1-pRUF, the CXCL12-, HIF-1 α - and HIF-2 α -overexpressing lines, LP-1-pFIV, scrambled RNAi control, and the CXCL12-, HIF-1 α - and HIF-2 α -knockdown lines. Each cell line was cultured under normoxic or hypoxic culture conditions for 72 hours and levels of CXCL12 protein expression measured using an ELISA. Graphical representation of these data illustrates changes in levels of CXCL12 protein detected in conditioned media collected from each cell line cultured under normoxic () and hypoxic () conditions, normalised to total cellular protein concentration. Data are expressed as mean \pm standard deviation from replicate samples of a representative experiment of three. *p<0.05 and **p<0.05, one-way ANOVA.

A



	Mean CXCL12 Conc. ± SEM <i>NORMOXIA</i>	Mean CXCL12 Conc. ± SEM <i>HYPOXIA</i>
pRUF	138.9 ± 11.7 pg/mL	502.2 ± 35.0 pg/mL
CXCL12	939.4 ± 25.3 pg/mL	1520.1 ± 43.2 pg/mL
HIF-1α	345.5 ± 26.7 pg/mL	606.8 ± 52.1 pg/mL
HIF-2α	432.6 ± 22.1 pg/mL	667.7 ± 52.4 pg/mL
pFIV	124.02 ± 13.6 pg/mL	395.68 ± 26.2 pg/mL
scram RNAi	133.70 ± 12.9 pg/mL	353.33 ± 29.4 pg/mL
CXCL12-KD	79.12 ± 9.5 pg/mL	163.45 ± 13.7 pg/mL
HIF-1α-KD	128.97 ± 16.1 pg/mL	208.53 ± 18.0 pg/mL
HIF-2α-KD	114.9 ± 8.6 pg/mL	172.22 ± 11.6 pg/mL

Figure 5.9. CXCR4 Expression in All Transduced LP-1 Cell Lines. Each of the transduced LP-1 cell lines created for this project was stained with an anti-CXCR4 monoclonal antibody and its corresponding isotype-matched negative control and levels of CXCR4 protein expression measured using flow cytometry. Filled histograms (■) indicate background fluorescence following staining with the isotype-matched negative control antibody. Unfilled histograms (▨) indicate levels of CXCR4 expression in (A) LP-1-pRUF, (B) LP-1-CXCL12, (C) LP-1-HIF-1 α , (D) LP-1-HIF-2 α , (E) LP-1-pFIV, (F) LP-1-CXCL12 RNAi, (G) LP-1-scrambled RNAi, (H) LP-1-HIF-1 α RNAi, and (I) LP-1-HIF-2 α RNAi cell lines. The mean fluorescence intensity for each stain is included above each histogram, and data from a representative experiment of three is shown.

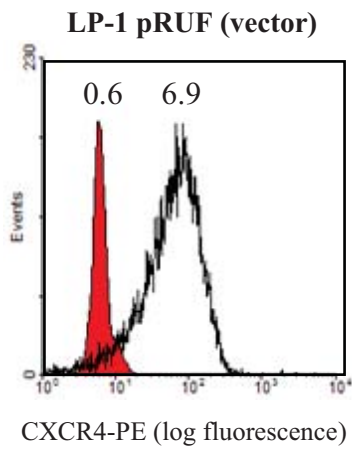
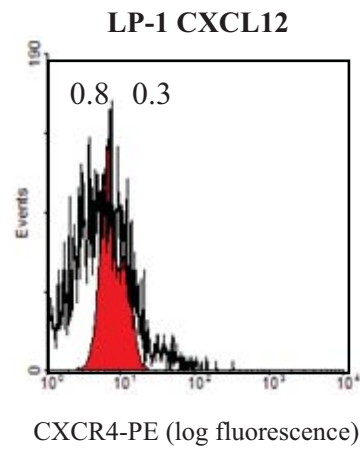
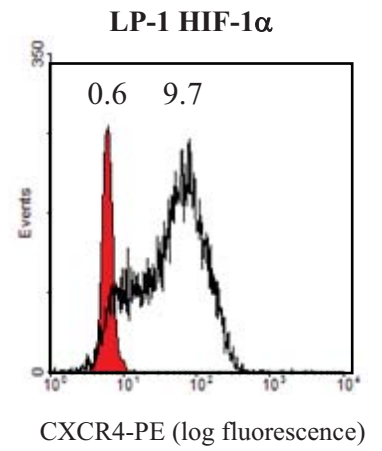
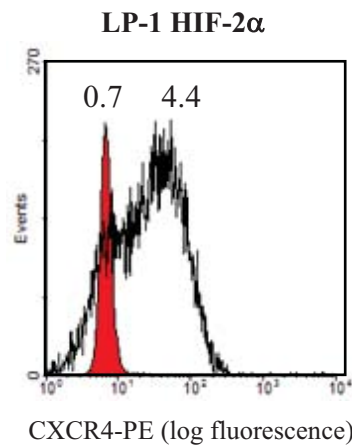
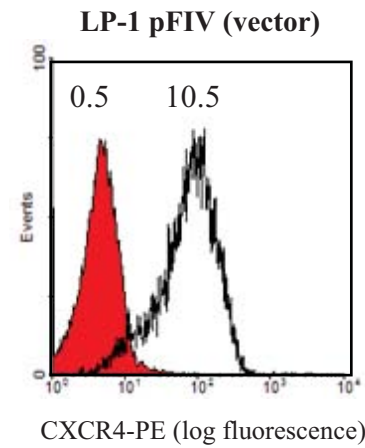
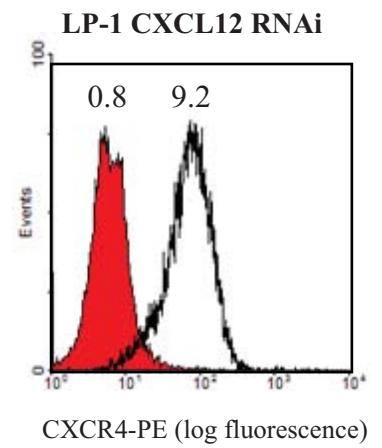
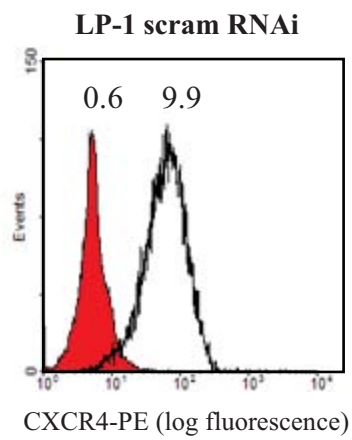
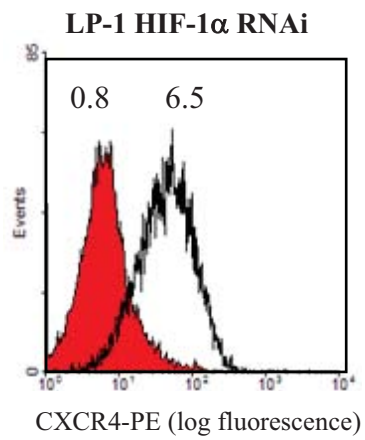
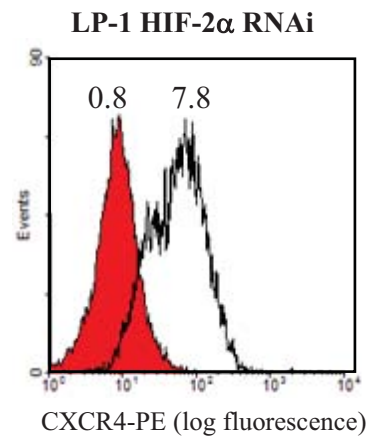
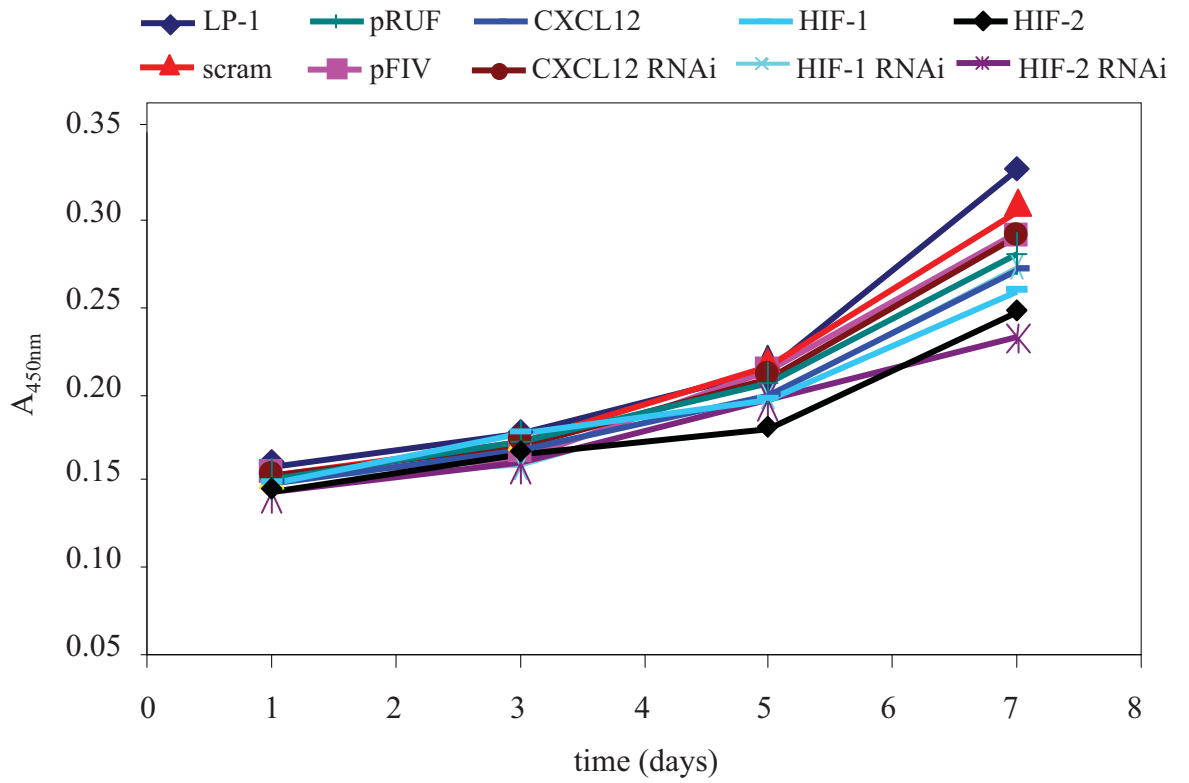
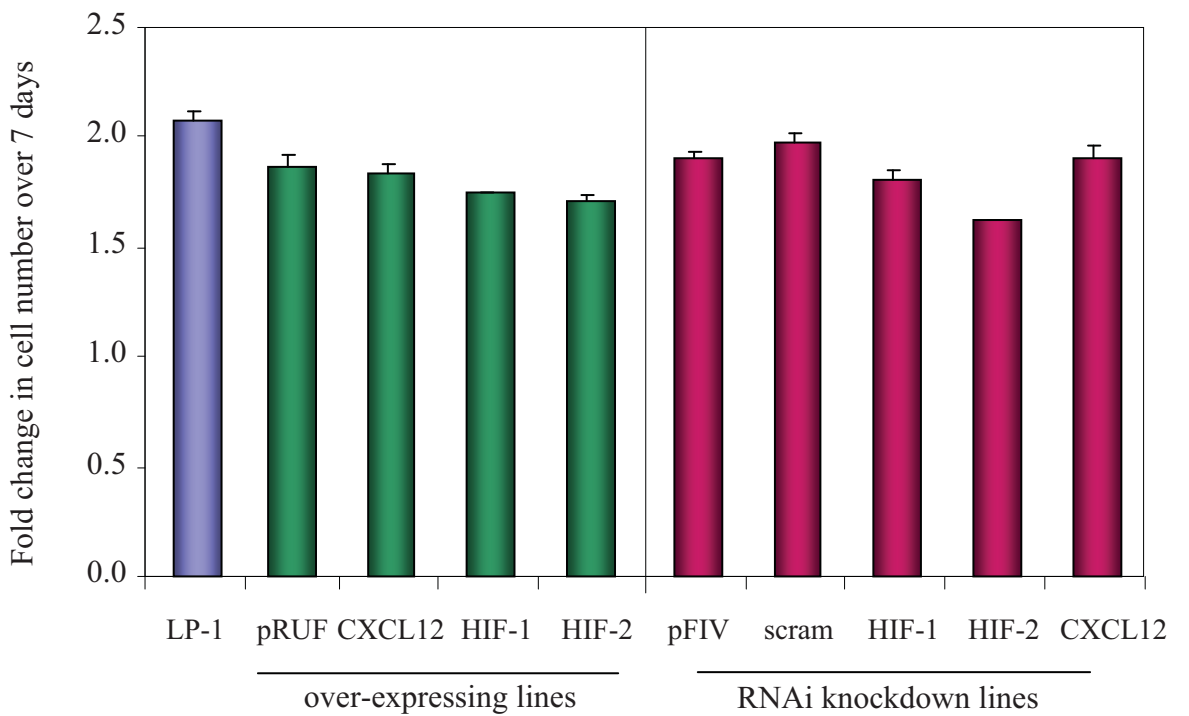
A**B****C****D****E****F****G****H****I**

Figure 5.10. A Comparison of the Rate of Proliferation of All Transduced LP-1 Cell Lines. All of the transduced LP-1 cell lines created for this project were seeded at a density of 4000 cells/ well in 96-well tissue culture plates using preparative cell sorting and cultured for 7 days. At day 1, 3, 5, and 7 time points, the number of viable, proliferating cells was assessed using WST-1 reagent. In (A), the cumulative WST-1 data is plotted for each cell line over the 7 day time course. In (B), the data is re-plotted to reflect the fold change in WST-1 absorbance at day 7 compared to the respective day 1, to better display the overall rates of proliferation over the 7 day period. Data are expressed as the mean \pm standard deviation of replicate samples of a representative experiment of three

A**B**

(Figure 5.10B). These data clearly illustrate that there is no significant difference in the proliferation rates of these transduced cell lines.

5.2.4 *In vivo* studies

5.2.4.1 *The role of CXCL12 in MM-induced angiogenesis*

To examine the role of CXCL12 in MM-induced angiogenesis in the *in vivo* mouse model described earlier (see Figure 5.5), LP-1-pRUF, LP-1-CXCL12, LP-1-pFIV and LP-1-CXCL12-KD cells were mixed with Matrigel matrix and implanted subcutaneously into immunocompromised nude mice. To facilitate bioluminescence monitoring, each of the cell lines was also co-transduced with the SFG_{NES}-TGL luciferase reporter construct. As a negative control, each mouse also received a Matrigel implant containing no cells. Tumour growth was monitored weekly for two weeks using *in vivo* bioluminescence imaging (Figure 5.11), and a time-dependent increase in bioluminescence signal intensity and diameter was observed in all mice (Figure 5.11).

To illustrate the level of MM cell line-induced angiogenesis, photographs were taken of each implant containing LP-1-pRUF cells (Figure 5.12A), LP-1-CXCL12 cells (Figure 5.12B), LP-1-pFIV cells (Figure 5.12C), and LP-1-CXCL12-KD cells (Figure 5.12D) and the corresponding negative control implants. The implants were then excised, weighed, and the haemoglobin content measured using the Drabkin's assay. Drabkin's data were normalised to the weight of the respective sample to give a relative assessment of vascularity, and then normalised to the bioluminescence signal intensity emitted from the implant at the time of sacrifice. This normalised the level of vascularity to the number of viable tumour cells present (Figure 5.12E). LP-1-CXCL12 cells induced a 5-fold increase in angiogenesis compared to the LP-1-pRUF vector control (Figure 5.12E, $p < 0.03$, one-way ANOVA). No significant difference in angiogenesis was observed LP-1-CXCL12-KD cells compared to the LP-1-pFIV vector control ($p = 0.7$, one-way ANOVA).

5.2.4.2 *The role of HIF-1 α and HIF-2 α in MM-induced angiogenesis, and the contribution of CXCL12 to this process.*

To examine the effect of HIF-1 α and HIF-2 α over-expression on MM-induced angiogenesis and the contribution of CXCL12 to this process, LP-1-pRUF, LP-1-CXCL12, LP-1-HIF-1 α and LP-1-HIF-2 α cells were implanted subcutaneously into immunocompromised nude mice (5×10^6 cells/ implant). To facilitate bioluminescence monitoring,

Figure 5.11. Bioluminescence Monitoring of the *In Vivo* Tumour Growth of LP-1 Cells Engineered to Over-Express or Knockdown CXCL12. LP-1-pRUF, LP-1-CXCL12, LP-1-pFIV and LP-1-CXCL12 RNAi cells were mixed in liquid Matrigel and injected subcutaneously into the right ventral flank of immunocompromised mice (5×10^6 cells/implant). As a negative control, a Matrigel implant containing no cells was implanted into the left ventral flank of each mouse. To facilitate *in vivo* bioluminescence monitoring, all of the cell lines used in this experiment were co-transduced with the SFG_{-NES}-TGL luciferase reporter construct. Using *in vivo* bioluminescence imaging, tumour growth was assessed at weekly intervals for two weeks following the administration of D-luciferin substrate. At each time point, pseudocolour bioluminescence images were recorded and overlaid onto grayscale photographs, and the bioluminescence intensity measured as photons/second/cm². These images are representative of animal cohorts containing six animals.

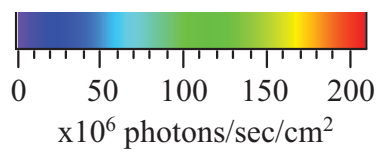
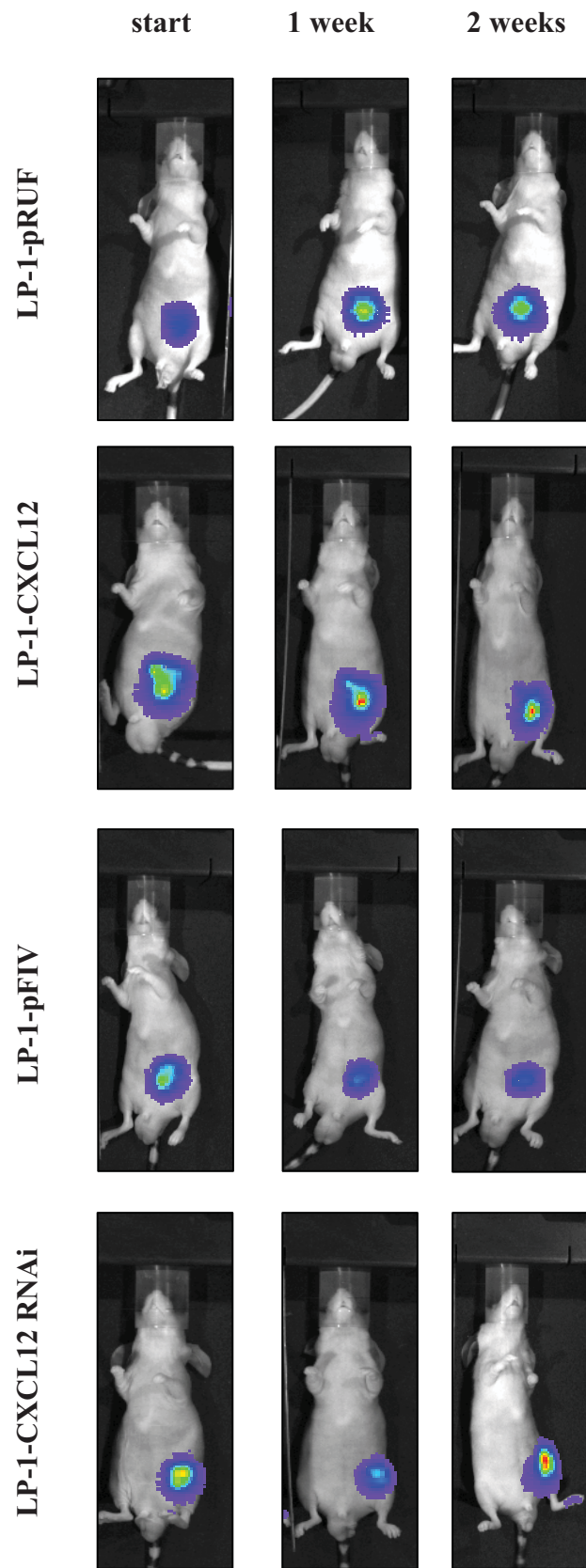


Figure 5.12. The Induction of *In Vivo* Angiogenesis by LP-1 Cells Engineered to Over-Express or Knockdown CXCL12. LP-1-pRUF, LP-1-CXCL12, LP-1-pFIV and LP-1-CXCL12 RNAi cells were mixed in liquid Matrigel and injected subcutaneously into the right ventral flank of immunocompromised mice (5×10^6 cells/ implant). As a negative control, each mouse also received a Matrigel implant containing no cells. After two weeks, the mice were humanely killed, and macroscopic photographs were taken of each implant. Representative photographs of negative control implants and corresponding cell implants containing (A) LP-1-pRUF, (B) LP-1-CXCL12, (C) LP-1-pFIV, and (D) LP-1-CXCL12 RNAi cells are shown, to illustrate the level of angiogenesis induced by each of these cells. (E) Following careful dissection of the implant from the surrounding tissue, implants were weighed and the haemoglobin content of each implant measured using the Drabkin's assay. Drabkin's data were normalised to the weight of each tissue sample, to give a relative determination of vascularity per milligram of sample. Data are expressed as mean \pm standard deviation from animal cohorts containing six animals. * $p < 0.03$, one-way ANOVA.

A**LP-1-pRUF**

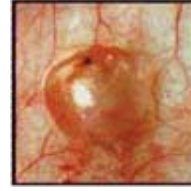
no cells



cells

**B****LP-1-CXCL12**

no cells



cells

**C****LP-1-pFIV**

no cells



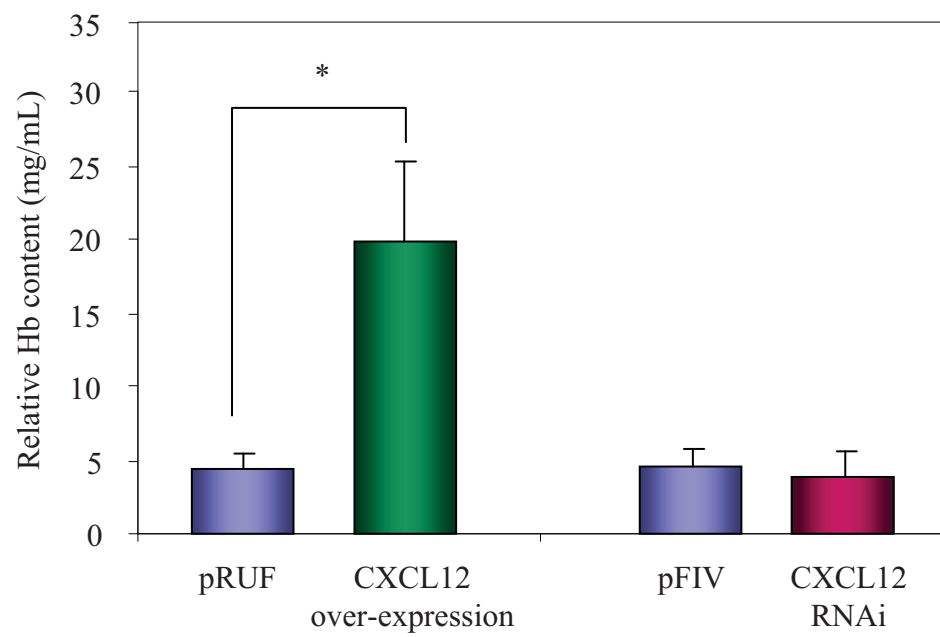
cells

**D****LP-1-CXCL12 RNAi**

no cells



cells

**E**

each of these cell lines were also co-transduced with the SFG_{NES}-TGL luciferase reporter construct. As a negative control, each mouse also received a Matrigel implant containing no cells. To examine the contribution of CXCL12/CXCR4 to angiogenesis induced by each of the over-expressing cell lines, Alzet pumps containing the CXCR4 antagonist, T140, were implanted subcutaneously into the upper dorsum of half of the mice in each group.

Tumour growth was monitored weekly for two weeks using *in vivo* bioluminescence imaging (Figure 5.13) and in all of the mice not receiving T140, a time-dependent increase in bioluminescence signal intensity and diameter was observed. A similar time-dependent increase in bioluminescence was also observed in mice receiving LP-1-pRUF cells + T140. However in contrast, mice receiving LP-1-CXCL12, LP-1-HIF-1 α and LP-1-HIF-2 α cells with T140 administration displayed a marked decrease in bioluminescence signal intensity and diameter compared to respective mice cohorts not receiving T140.

To illustrate the level of angiogenesis induced by each of the different cell lines after two weeks, photographs were taken of cell implants containing LP-1-pRUF cells (Figure 5.14A), LP-1-pRUF cells + T140 (Figure 5.14B), LP-1-CXCL12 cells (Figure 5.14C), LP-1-CXCL12 cells + T140 (Figure 5.14D), LP-1-HIF-1 α cells (Figure 5.14E), LP-1-HIF-1 α cells + T140 (Figure 5.14F), LP-1-HIF-2 α cells (Figure 5.14G) and LP-1-HIF-2 α cells + T140 (Figure 5.14H), and the corresponding negative control implants.

The implants were then excised, weighed, and haemoglobin content measured using the Drabkin's assay (Figure 5.15). A significant increase in angiogenesis was observed in implants containing LP-1-CXCL12, LP-1-HIF-1 α and LP-1-HIF-2 α cells compared to the LP-1-pRUF vector control (Figure 5.15, $p < 0.05$, one-way ANOVA). Furthermore, a significant decrease in angiogenesis was observed in mice which received LP-1-CXCL12 implants + T140, compared to mice which received LP-1-CXCL12 implants without T140 (Figure 5.15, $p < 0.05$, one-way ANOVA). While a decrease in angiogenesis was also observed in mice receiving LP-1-HIF-1 α and LP-1-HIF-2 α cells and T140 compared to those that did not receive T140, statistical significance was not achieved ($p = 0.06$, one-way ANOVA).

Figure 5.13. Bioluminescence Monitoring of the *In Vivo* Tumour Growth of CXCL12-, HIF-1 α - or HIF-2 α - Over-Expressing LP-1 Cells in the Presence or Absence of T140.

LP-1 cells engineered to over-express CXCL12, HIF-1 α or HIF-2 α and the respective pRUF vector control were mixed in liquid Matrigel and injected subcutaneously into the right ventral flank of immunocompromised mice (5×10^6 cells/ implant). As a negative control, a Matrigel implant containing no cells was implanted into the left ventral flank of each mouse. To facilitate bioluminescence monitoring, all of the cell lines used in this experiment were co-transduced with the SFG_{NES}-TGL luciferase reporter construct. To examine the contribution of CXCL12 to the amount of angiogenesis induced by each cell line, Alzet pumps containing the CXCR4 antagonist, T140, were subcutaneously implanted into the dorsal flank of half of the mice in each group two days prior to cell implantation. Using *in vivo* bioluminescence imaging, tumour growth was assessed at weekly intervals for two weeks following the administration of D-luciferin substrate. At each time point, pseudocolour bioluminescence images were recorded and overlaid onto grayscale photographs, and the bioluminescence intensity measured as photons/second/cm². These images are representative of animal cohorts containing five animals.

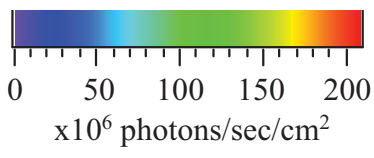
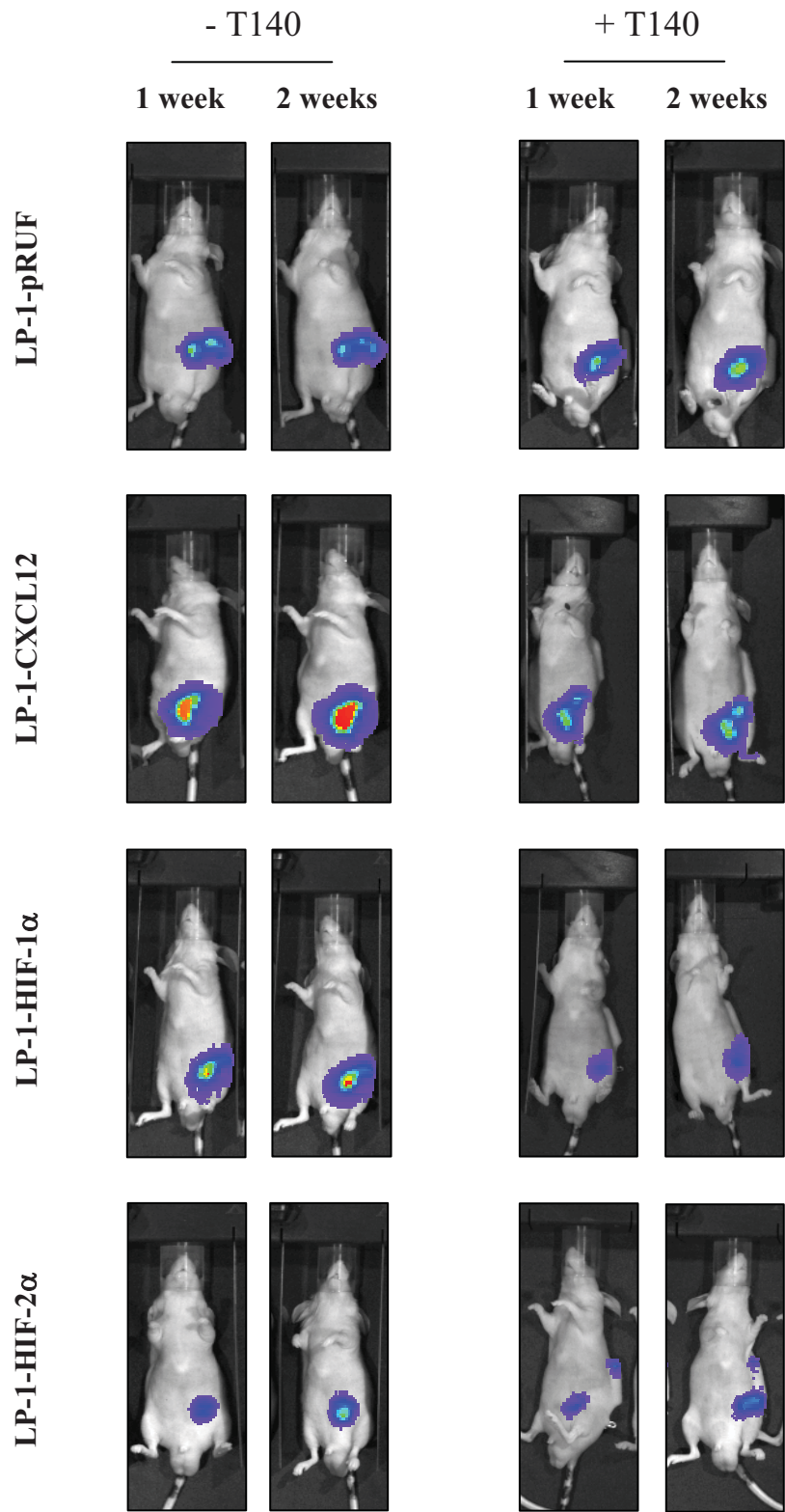


Figure 5.14. The Induction of *In Vivo* Angiogenesis by LP-1 Cells Engineered to Over-Express CXCL12, HIF-1 α or HIF-2 α in the Presence or Absence of T140. LP-1-pRUF, LP-1-CXCL12, LP-1-HIF-1 α and LP-1-HIF-2 α cells were mixed in liquid Matrigel and injected subcutaneously into the right ventral flank of immunocompromised mice (5×10^6 cells/implant). As a negative control, a Matrigel implant containing no cells was implanted into the left ventral flank of each mouse. To examine the contribution of CXCL12 to the amount of angiogenesis induced by each cell line, Alzet pumps containing the CXCR4 antagonist, T140, were subcutaneously implanted into the dorsal flank of half of the mice in each group two days prior to cell implantation. After two weeks, the mice were humanely killed, and macroscopic photographs were taken of each implant. Representative photographs of negative control implants and corresponding cell implants containing (A) LP-1-pRUF, (B) LP-1-pRUF + T140, (C) LP-1-CXCL12, (D) LP-1-CXCL12 + T140, (E) LP-1-HIF-1 α , (F) LP-1-HIF-1 α + T140, (G) LP-1-HIF-2 α , and (H) LP-1-HIF-2 α + T140 are shown, to illustrate the level of angiogenesis induced by each of these cells in the presence or absence of T140. These images are representative of animal cohorts containing five animals.

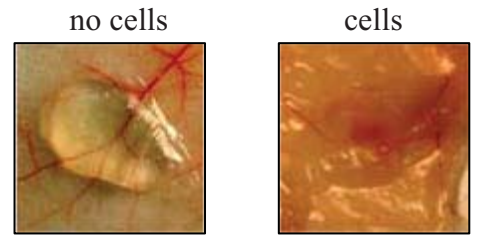
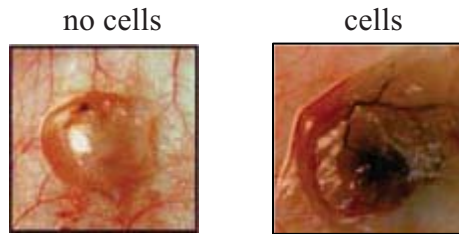
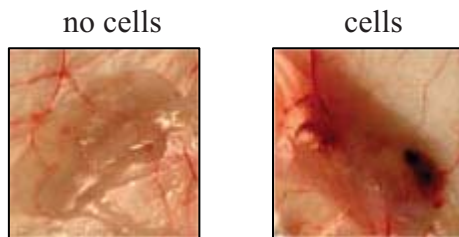
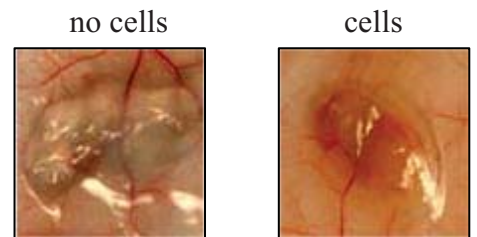
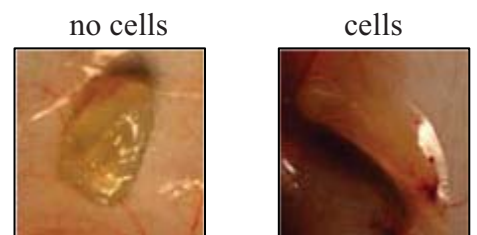
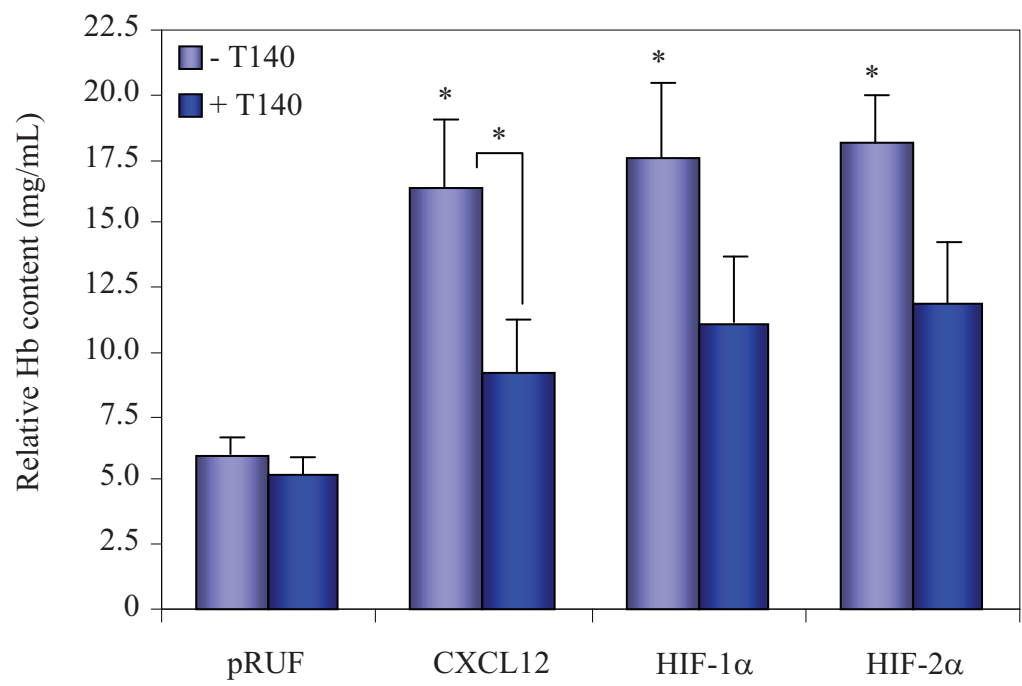
ALP-1-pRUF**B**LP-1-pRUF + T140**B**LP-1-CXCL12**D**LP-1-CXCL12 + T140**C**LP-1-HIF-1 α **F**LP-1-HIF-1 α + T140**D**LP-1-HIF-2 α **H**LP-1-HIF-2 α + T140

Figure 5.15. Drabkin's Assessment of *In Vivo* Angiogenesis Induced by LP-1 Cells Engineered to Over-Express CXCL12, HIF-1 α or HIF-2 α in the Presence or Absence of T140. Following careful dissection of the implant from the surrounding tissue, implants were weighed and the haemoglobin content of each implant measured using the Drabkin's assay. Graphical representation of these data demonstrate the average relative haemoglobin content of cell implants in the absence of T140 (■) and presence of T140 (■). Data are expressed as mean \pm standard deviation from animal cohorts containing five animals. * $p < 0.05$, one-way ANOVA



5.3 Summary and Discussion

In MM, the molecular mechanisms responsible for the progressive increase in BM angiogenesis remain unclear. This is due, in large part, to the complexity of interactions between tumour cells and host cells, and the secretion of an array of pro-angiogenic chemokines, cytokines, growth factors and enzymes. In studies presented in the preceding chapters, the ability of MM-derived CXCL12 to stimulate *in vitro* tube formation and the role of hypoxia and the HIF transcription factors in regulating CXCL12 and CXCR4 expression in MM PCs was examined. While these *in vitro* investigations provided important insights into the role of CXCL12 in MM, *in vivo* studies were performed to confirm these findings. In studies presented in this chapter, the *in vivo* Matrigel plug assay was used to assess the ability of CXCL12 to stimulate angiogenesis *in vivo*, and the contribution of the HIF-1 and HIF-2 transcription factors to this process.

To date, a number of different models have been used to investigate MM-induced angiogenesis *in vivo*. In the 5T2MM and 5T33MM systemic mouse models, BM MVD has been assessed in the long bones, ribs and vertebrae using CD31 immunohistochemical staining of BM vasculature^{260,368,485}. The chick embryo CAM assay has been used to demonstrate the ability of MM PCs to induce significant capillary growth and an increase in microvessel area^{412,486}. In a subcutaneous xenograft model, the Matrigel plug assay has been used to examine the ability of putative anti-angiogenic agents such as pazopanib⁴⁸⁷, CCI-779⁴⁸⁸ and enzastaurin⁴⁸⁹ to reduce MM-induced angiogenesis.

While repeated attempts were made to assess *in vivo* angiogenesis in the murine BM microenvironment, an alternative approach was sought due to the difficulty in assessing BM MVD by immunohistochemical methods. A subcutaneous Matrigel xenograft model, which has previously been used to assess MM-induced angiogenesis⁴⁸⁷⁻⁴⁸⁹, was chosen due to its relative simplicity, reproducibility and limited invasiveness. Although the subcutaneous space is a well-studied site of tumour growth^{226,242,364,487-492}, it has a number of intrinsic characteristics that set it apart from other sites throughout the body. These include a lack of spatial constraints in the form of matrix or skeletal elements and relatively sparse vascularisation³⁶⁴. However, while the subcutaneous environment is not the typical site for MM-induced angiogenesis in the clinical setting, the Matrigel xenograft model has a key advantage over other *in vivo* angiogenesis models in that it is able to replicate the hypoxic BM microenvironment⁴²¹. On this basis, the Matrigel xenograft

model was considered the most suitable alternative to the intramedullary disease approach for studying MM-induced tumour angiogenesis.

In previous studies using the subcutaneous Matrigel xenograft model, MM cells were implanted at concentrations ranging between 1×10^7 and 3×10^7 cells/ implant and allowed to grow until the tumour reached a size of 2 centimetres⁴⁸⁷⁻⁴⁸⁹. In contrasting studies presented here, substantial levels of necrosis and cell death were observed following the implantation of 1×10^7 LP-1 cells, as assessed by *in vivo* bioluminescence imaging of tumour cell viability, and tumours failed to reach sizes of 2 centimetres over the 5 week period. These findings likely reflect phenotypic differences between the MM PC lines used. As angiogenesis is generally assessed at 10 – 20 days after implantation in the Matrigel xenograft model^{492,493} and based on the kinetics of tumour cell growth observed in these preliminary titration studies, 5×10^6 cells/ implant was considered the optimal cell number for a 14-day assessment of angiogenesis and was used for all subsequent experiments.

To assess the ability of MM PC-derived CXCL12 to induce tumour angiogenesis *in vivo*, modified LP-1 cells over- or under-expressing CXCL12 were implanted into the subcutaneous Matrigel xenograft model. While studies presented in Chapter 3 showed that LP-1 MM PCs alone express strong endogenous levels of CXCL12, the level of this expression is still much lower than that observed in patient-derived CD38⁺ MM PCs. Therefore, to better reflect the CXCL12 levels observed in MM patients, CXCL12 over-expressing LP-1 cells were used in these studies. Importantly, a statistically significant increase in angiogenesis was induced by these cells compared to the vector control, and the RNAi-mediated suppression of CXCL12 completely abolished this response. These data clearly demonstrate that MM-derived CXCL12 induces *in vivo* angiogenesis. Given that LP-1 cells themselves express CXCL12, it was somewhat surprising that the RNAi-mediated knockdown of CXCL12 in these cells did not elicit a greater reduction in angiogenesis compared to the vector control. One possible explanation for this observation is the relative insensitivity of this *in vivo* assay and the surrogate method used to assess angiogenesis.

In a recent report by Menu *et al*²⁶⁰, the stimulation of murine 5T2MM and 5T33MM cells with CXCL12 *in vitro* resulted in a 20% increase in the rate of cellular proliferation. To

determine whether the increased angiogenesis induced by CXCL12 was attributed to a cell growth advantage, the proliferation rates of LP-1 cells over- or under-expressing CXCL12 were examined. In these *in vitro* studies, MM PC proliferation was not affected by endogenous CXCL12, and parental LP-1 cells were unaffected by exogenous rhCXCL12 (data not shown). These observations confirm those of Hideshima *et al*²⁶⁸, who showed that CXCL12 stimulates only modest increases in the proliferation of MM PC lines and primary MM patient cells. Furthermore, studies by Libura *et al*⁴³⁵ have showed that not all CXCR4-expressing tumour cells proliferate in response to CXCL12.

The ability of MM-derived CXCL12 to stimulate angiogenesis was confirmed in a subsequent *in vivo* study, in which CXCL12 over-expressing LP-1 cells were implanted in mice in the presence or absence of the CXCR4 antagonist, T140. Again, the CXCL12 over-expressing LP-1 cells strongly induced angiogenesis in our mouse model, and the administration of T140 mediated a statistically significant decrease in angiogenesis. Together, these studies confirm the *in vitro* studies presented in Chapter 3 and demonstrate that MM-derived CXCL12 stimulates tumour angiogenesis *in vivo*.

These *in vivo* findings complement previous studies which have shown that tumour-derived CXCL12 mediates angiogenesis in ovarian cancer²⁴⁷, gastrointestinal tumours⁴⁷⁸, prostate cancer^{226,494}, basal cell carcinoma⁴⁹⁵, colorectal cancer⁴⁸⁰ and breast cancer^{242,479}. However, in the context of MM, our data directly contradicts findings published by Menu *et al*²⁶⁰, who showed that the administration of T140 had no effect on BM MVD in myelomatous 5T33MM mice. However, the 5T33MM cells used in this study did not express CXCL12, and therefore the ability of MM-derived CXCL12 to stimulate angiogenesis was not under direct investigation. Using two different approaches, namely CXCL12 over-expression vs. CXCL12 knockdown and CXCL12 over-expression in the presence or absence of T140, the data presented here clearly shows that MM-derived CXCL12 induces *in vivo* angiogenesis.

Levels of HIF-1 α and HIF-2 α protein expression in patient biopsy specimens directly correlate with MVD in bladder cancer^{359,496}, lung cancer³⁵⁴, osteosarcoma⁴⁹⁷, hepatocellular carcinoma⁴⁹⁸, prostate cancer⁴⁹⁹, gastric carcinoma⁵⁰⁰, colorectal carcinoma⁵⁰¹, chondrosarcoma⁵⁰², rectal cancer⁵⁰³, clear cell renal cell carcinoma⁵⁰⁴, nasopharyngeal carcinoma⁵⁰⁵ and ovarian cancer⁵⁰⁶. Experimentally, using tumour cell

lines in which HIF-1 α or HIF-2 α have been over-expressed or knocked down, the subcutaneous xenograft model has been used to examine the role of HIF-1 and HIF-2 in tumour angiogenesis induced by neuroblastoma⁴⁶³, renal cell carcinoma^{459,507,508}, bladder cancer⁵⁰⁷, and colon cancer⁵⁰⁹. To examine the effect of HIF-1 α and HIF-2 α over-expression in MM-induced angiogenesis in our *in vivo* mouse model and the contribution of CXCL12 to this process, LP-1-pRUF, LP-1-CXCL12, LP-1-HIF-1 α and LP-1-HIF-2 α cells were subcutaneously implanted into mice and half of the mice in each group were treated with the CXCR4 antagonist, T140. While not statistically significant, the administration of T140 markedly reduced the level of *de novo* angiogenesis induced by HIF-1 α - and HIF-2 α -over-expressing cell lines, demonstrating that CXCL12 is involved in HIF-induced angiogenesis *in vivo*. In addition to CXCL12, a number of other pro-angiogenic cytokines and growth factors are up-regulated by hypoxia, including VEGF^{373,374}, Ang-2^{375,376}, bFGF³⁷⁷, PDGF^{377,378}, endothelin-1³⁷⁹, and TNF α ³⁸⁰.

In this study, a marked decrease in bioluminescence signal intensity and diameter was observed in response to T140 in mice harbouring LP-1-CXCL12, LP-1-HIF-1 α and LP-1-HIF-2 α cell implants. This effect was not observed in the vector control group, and while this could indicate that CXCL12 is involved in tumour cell survival, it most likely reflects a decrease in tumour survival occurring as a consequence of decreased angiogenesis and deprivation of oxygen and nutrients. Interestingly, compared to the other animal cohorts, a substantial decrease in tumour cell viability was observed in the mice that received LP-1-HIF-2 α implants, both in the presence and absence of T140. This can not be explained by a difference in cell proliferation, as *in vitro* studies revealed no difference in proliferation rates of these cell lines. The effect of HIF-2 α over-expression on *in vivo* tumour growth remains unclear, as several studies have reported contradictory findings. Our observations agree with those of Blancher *et al*⁵¹⁰, who showed that HIF-2 α over-expressing MDA-435 breast cancer cells exhibit impaired subcutaneous tumour growth compared to the vector control in the absence of any difference in *in vitro* growth characteristics between these cells. However, over-expression of HIF-2 α in renal cell carcinoma⁴⁵⁹ and neuroblastoma⁴⁶³ cell lines has been shown to impart a substantial *in vivo* growth advantage to tumour cells. These conflicting data can be attributed to differences in the tumour cell types studied, and/or relate to the different subsets of HIF target genes that are induced in these cells.

In summary, the *in vivo* studies presented in this chapter demonstrate that MM-derived CXCL12 induces tumour angiogenesis and that CXCL12 is involved in HIF-induced angiogenesis *in vivo*. The clinical significance of these findings will be discussed in detail in the final discussion.

Chapter 6:

GENERAL DISCUSSION

6.1 Summary & General Discussion

MM is an incurable haematological malignancy characterised by the clonal proliferation of malignant PCs within the BM. MM accounts for approximately 1% of all cancers and is the second most common haematological malignancy after NHL^{16,25}. Each year in Australia, approximately 1,100 people are diagnosed with MM, almost 80% of whom are over the age of 60²⁵. Alarming, the latest national statistics reported a 44% increase in the number of Australians diagnosed with MM in 2003 compared to 1993²⁵.

The main clinical manifestations of MM are the development of devastating osteolytic bone lesions at multiple sites throughout the skeleton, bone pain, hypercalcemia, renal insufficiency, suppressed immunoglobulin production and increased BM angiogenesis¹⁶. Angiogenesis, or the formation of new blood vessels from pre-existing vasculature, is a hallmark of tumour progression in both solid⁹⁴⁻¹⁰⁴ and haematological^{4,6-8,105-114} malignancies.

Like many tumour cells, MM PC survival and expansion is dependent upon an adequate supply of oxygen and nutrients. Therefore, the acquisition of an angiogenic phenotype is one of the key malignant changes associated with the progression from MGUS and indolent MM to active MM^{4,6-8} (Figure 6.1). Furthermore, aberrant proliferation of MM PCs in the BM creates discrete regions of hypoxia, which further stimulate the production of angiogenic cytokines, including VEGF^{120,121,511}, bFGF⁴¹², HGF¹²⁶ and Ang-1⁸⁴. Soluble levels of these factors have been shown to be elevated in the BM and PB circulation of MM patients^{122,125-127,512-515}. In addition to producing angiogenic growth factors and cytokines themselves, MM PCs also induce their production by surrounding microenvironmental cells such as BMSCs and ECs. Neutralisation of the biological activity of any one of these factors is insufficient to abolish MM-induced angiogenesis *in vitro* and *in vivo*^{134,516}. This reflects the complexity of tumour angiogenesis, and the many angiogenic stimuli which act collectively to mediate this process.

There is now a considerable body of data demonstrating that CXCL12 has multiple functions in vascular remodelling. *In vitro* studies have showed that the binding of CXCL12 to EC-expressed CXCR4 induces EC survival²⁵⁴, proliferation^{254,260}, chemotaxis^{10,177,178,203,260,480}, and tube formation^{10,12,495}. The ability of CXCL12 to stimulate angiogenesis *in vivo* has been demonstrated in the rabbit corneal micropocket

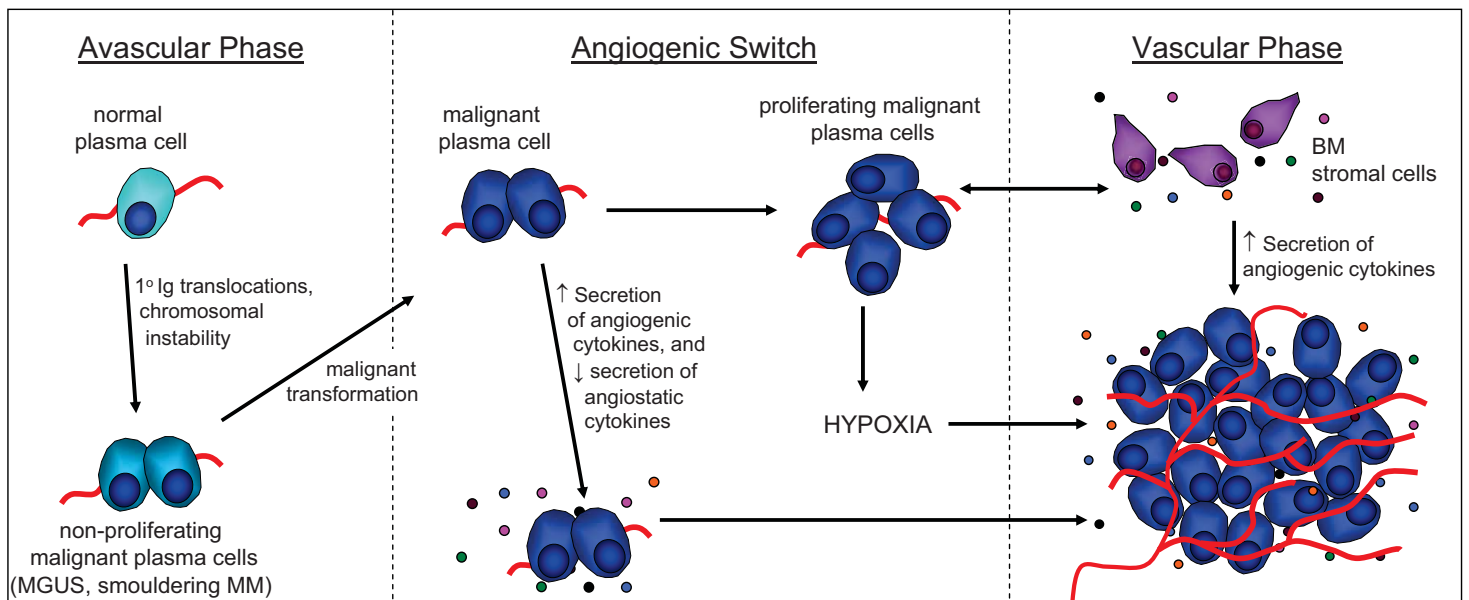


Figure 6.1. The Angiogenic Switch in Multiple Myeloma. Initial chromosomal events which transform normal PCs into non-proliferating malignant PCs (ie. in MGUS and smoldering MM) are insufficient to activate the angiogenic switch, thus retaining the cells in a dormant, avascular state. Subsequent chromosomal translocations complete the malignant transformation, causing the concomitant induction of angiogenic cytokines and suppression of angiostatic cytokines. The hypoxic bone marrow microenvironment, coupled with paracrine interactions between MM PCs and BMSCs, accelerate disease progression by increasing the production of angiogenic growth factors and cytokines such as VEGF and CXCL12 and promote the recruitment of additional blood vessels. Figure adapted with permission ¹¹⁹.

assay¹⁴, subcutaneous models^{10,226,242,247,256-258,478,479,494,495}, and the dorsal skinfold chamber⁴⁸⁰. In addition, CXCL12 indirectly induces angiogenesis by modulating tumour cell expression of other angiogenic factors such VEGF, IL-6, and IL-8^{494,495,517-519}. Interestingly, studies by Zhang *et al* have shown that MM patients have significantly higher numbers of circulating ECs and EC progenitors compared to healthy subjects⁵²⁰. In line with this, recent data also shows that CXCL12 is involved in adult vasculogenesis, with elevated PB levels of CXCL12 stimulating the mobilization and engraftment of CXCR4⁺ BM haemopoietic stem cells and EC progenitors into adult vasculature⁵²¹⁻⁵²³. The relative contributions of vasculogenesis and angiogenesis to the enhanced BM neovascularisation in MM are yet to be fully determined.

As illustrated by immunohistochemical analyses performed on patient bone biopsies in this project, MM PCs strongly express CXCL12. Furthermore, circulating PB levels of CXCL12 are significantly higher in MM patients compared to MGUS patients and age-matched healthy individuals. Previous studies have showed that CXCL12 is an important mediator of several key aspects of MM biology, including transendothelial migration^{164,264,265}, MM PC migration and retention within the BM^{168,192,260,266,267}, partial protection from dexamethasone-induced apoptosis²⁶⁸, and osteoclastic bone resorption⁹. Using CM from the MM PC line RPMI-8226 in the presence or absence of the specific CXCR4 antagonist, T140, we now show for the first time that MM PC-derived CXCL12 also stimulates *in vitro* tube formation. These *in vitro* findings were subsequently confirmed *in vivo*, using an established murine model of subcutaneous tumour angiogenesis. When CXCL12 over-expressing MM PCs were implanted into mice, a 2.5-fold increase in angiogenesis was observed, and the administration of the CXCR4 antagonist, T140, significantly reduced this response. These results complement previous studies performed in other tumour models, which have shown that tumour-derived CXCL12 mediates angiogenesis in gastrointestinal tumours⁴⁷⁸, prostate cancer²²⁶, colorectal cancer⁴⁸⁰ and breast cancer^{242,479}.

Interestingly, in addition to increased CXCL12 expression in MM PCs, previous studies by Al Rayes *et al*²⁶¹ have shown that MM PCs also exhibit more than twice the level of CXCR4 receptor expression compared to normal and MGUS PCs. While the progression from MGUS to MM is associated with an increase in both CXCL12 and CXCR4 expression, the biological significance of this is currently unknown. Studies presented in

this thesis demonstrate that increased MM PC expression of CXCL12 and CXCR4 is, in part, the result of cellular adaptation to hypoxic conditions within the BM environment. Hypoxia, a state in which cells or tissues are deprived of oxygen, initiates cell-specific transcription programs to coordinate the expression of hundreds of gene products. The hypoxic regulation of CXCL12 has been reported in numerous other cell types^{15,247,390,391}, and the HIF-1 transcription factor identified as the mediator of this response^{15,391}.

While our studies confirmed that HIF-1 also regulates CXCL12 expression in MM PCs under hypoxic conditions, we found that HIF-2 is the predominant mediator of this response and showed that HIF-2 is able to bind directly to the CXCL12 promoter under hypoxic conditions. The ability of HIF-induced MM PC-derived CXCL12 to stimulate *in vivo* angiogenesis was subsequently confirmed using our established Matrigel xenograft model. When HIF-1 α - or HIF-2 α - over-expressing MM PCs were implanted subcutaneously into mice, a 2.5-fold increase in angiogenesis was observed, and administration of the T140 antagonist to these mice markedly reduced this response. This reduction in HIF-induced angiogenesis in the presence of T140 was not statistically significant, reflecting the fact that other angiogenic growth factors are also involved in HIF-induced angiogenesis. These results complement previous studies performed in other tumour models, which show that HIF over-expression mediates angiogenesis in neuroblastoma⁴⁶³, renal cell carcinoma^{459,507,508}, bladder cancer⁵⁰⁷, and colon cancer⁴¹⁵. However, to the best of our knowledge, our study is the first to examine the contribution of a single angiogenic growth factor in HIF-induced angiogenesis *in vivo*.

6.2 Therapeutic Implications of These Findings

Following Judah Folkman's pioneering observation that progressive tumour growth is dependent on the ability to induce additional blood supply⁹¹, over 10,000 research papers have been published in the field of angiogenesis. The culmination of this research is the development of several anti-angiogenic therapies which are currently undergoing various phases of pre-clinical and clinical testing. Preliminary results using anti-angiogenic agents such as bevacizumab, sunitinib and sorafenib⁵²⁴⁻⁵²⁶, which are being trialled in various combinations with different agents in several human cancers, have confirmed the relevance of this therapeutic approach and accelerated the search for novel, more potent drugs.

The majority of leading anti-angiogenic strategies have focussed on inhibiting the actions of VEGF. However, it is becoming increasingly clear that the inhibition of a single growth factor or pathway is insufficient to adequately overcome tumour angiogenesis, due to the existence of multiple growth factors and signalling pathways and the ability of tumour cells to adapt and exploit alternative mechanisms and growth pathways. Given the accumulating evidence implicating CXCL12 in angiogenesis and vasculogenesis, the potential anti-angiogenic benefit of CXCL12/CXCR4 antagonists such as AMD-3100^{427,428}, T134⁴²⁹, CTCE-9908^{527,528} and T140^{430-432,436} appears promising. Studies to date have confirmed that AMD3100 administration to mice efficiently blocks CXCL12-mediated mobilisation of CXCR4⁺ BM precursor cells and impairs ischemic vasculogenesis *in vivo*⁵²⁹, and inhibits VEGF-induced mobilization of CXCR4⁺ cells from the BM by reducing retention of these cells at the target site and inhibiting *in situ* EC proliferation⁵³⁰. Furthermore, AMD-3100 has been shown to reduce tumour growth and vascularisation in intracranially- and subcutaneously-implanted gliomal cells⁵²³. Similarly, T140 administration to mice harbouring subcutaneously implanted breast cancer cells significantly reduces tumour growth and angiogenesis⁴⁷⁹.

Interestingly, several studies have demonstrated that CXCL12 and VEGF act synergistically to mediate angiogenesis^{247,523,529-531}. While the mechanisms by which this occurs remain unclear, they are likely to involve both overlapping and mutually exclusive pathways. Given that CXCL12 and VEGF appear to be powerful angiogenic agents^{247,523,529-532}, the development of combined strategies which target both of these molecules and/or their receptors may have a significant advantage over current therapies targeting VEGF alone. However, further research is required to decipher the angiogenic CXCL12/CXCR4 and VEGF/VEGFR signalling pathways and define the mechanisms by which these molecules work together to augment angiogenesis.

In the context of MM, the potential ability of CXCL12/CXCR4 antagonists to inhibit other aspects of this disease, such as osteolytic bone resorption, is incredibly appealing⁹. However, CXCR4 is widely expressed throughout the body, which endows CXCL12 with the capacity to affect a broad range of cells. Therefore, with the potential for numerous side-effects resulting from systemic CXCL12/CXCR4 inhibition, pending results from current preclinical and clinical trials will provide valuable information as to the viability of this therapeutic strategy.

6.2.1 Will anti-angiogenic therapies live up to expectation?

While anti-angiogenic therapies clearly have the potential to improve patient outcomes, their use creates an interesting paradox. According to our current understanding of angiogenesis, the destruction of tumour vasculature would severely compromise oxygen delivery to tumour cells, thereby rendering them more hypoxic. Given that hypoxia is a strong pathophysiological stimulus for angiogenesis, this would instigate a vicious, never-ending cycle of reduced tumour vascularisation followed by subsequent hypoxia-induced revascularisation. Furthermore, tumour-associated hypoxia adversely favours tumorigenesis by conferring resistance to radiation and chemotherapeutic drugs, inducing genetic instability and serving as a selective pressure for tumour cells with increased metastatic potential⁵³³. In spite of this, emerging evidence suggests that, rather than depriving tumour cells of oxygen and increasing tumour hypoxia, anti-angiogenic agents transiently “normalise” the disorganised, leaky tumour vasculature and enhance oxygen and drug delivery to tumour cells^{534,535}.

Extensive research is still required to determine the optimal treatment guidelines for anti-angiogenic agents. While the combined administration of these drugs with traditional cytotoxic chemotherapeutics appears promising⁵³⁶, optimal scheduling of anti-angiogenic agents with chemotherapy requires a greater understanding of the time frame in which tumour normalisation occurs and how long it lasts. Furthermore, the dose and administration schedule for anti-angiogenic drugs is constrained by the delicate balance between vessel normalisation and excessive vascular regression. Sub-optimal doses might lower tumour oxygenation and antagonise rather than augment the response to cytotoxic agents, and excessive doses are likely to adversely affect the vasculature of normal tissues and increase the incidence of adverse effects⁵³⁵.

6.3 Future Directions

As discussed in Chapter 5, angiogenesis is best examined *in vivo* so as to account for interactions between environmental stimuli provided by the host and exogenous stimuli provided by the implant. As human cells are commonly implanted into mice, immunocompromised animals must be used to prevent rejection of the implanted cells. However, host immune cells such as monocytes, macrophages and dendritic cells are believed to be crucial microenvironmental contributors to angiogenesis⁵³⁷, and therefore the absence of these cells in immunocompromised mice is a key limitation of these animal

models. To avoid the need for using immunocompromised mice, syngeneic murine MM models have been developed. The 5T models of MM, namely 5T2MM, 5T33MM and 5TGM1, involve the injection of murine MM PCs, derived from myelomatous C57BL/KaLwRij mice, into immunocompetent recipient mice⁵³⁸⁻⁵⁴². While the 5T2MM and 5T33MM models require serial propagation of MM PCs from animal to animal, the 5TGM1 MM cell line permits *in vitro* propagation of MM PCs for transplantation⁵⁴³⁻⁵⁵⁰. In future studies, the 5TGM1 cell line will be stably transduced to over-express or knock down HIF-1 α , HIF-2 α and CXCL12, and the subsequent injection of these cells into immunocompetent mice will facilitate a more complete examination of the angiogenic properties of CXCL12 and the HIF transcription factors.

In light of recent data demonstrating that CXCL12 binds to the newly de-orphanised receptor, CXCR7²⁰⁹⁻²¹¹, further studies are required to examine the contribution of CXCR7 activation to CXCL12-induced angiogenesis. While the functional significance of CXCR7 is still under investigation, it has been shown to be expressed by ECs and tumour vasculature^{210,551}. Interestingly, the binding of CXCL12 to CXCR7 is believed to potentiate CXCL12-induced signalling through CXCR4²¹¹ which, given the importance of this chemokine pair to MM biology, highlights the need to investigate CXCR7. Future studies examining the expression of CXCR7 by patient-derived MM PCs and the consequences of blocking CXCL12/CXCR7 interactions on processes such as angiogenesis and osteoclastogenesis will provide much-needed insights into the biological importance of CXCR7 in MM.

The recent development of novel therapeutic agents such as, Lenalidomide and Bortezomib and the discovery of anti-angiogenic properties of Thalidomide has revolutionised patient outcomes. While these drugs are known to inhibit angiogenesis^{45,132,552-554}, the mechanisms by which they do so are not completely understood. To date, the effect of these drugs on interactions between CXCL12 and CXCR4 has not been investigated, and this represents another future direction of this project. Interestingly, a study published earlier this year reported that Bortezomib inhibits tumour adaptation to hypoxia by repressing HIF-1, and proposed that the anti-angiogenic effects of Bortezomib are the result of decreased hypoxia-induced angiogenesis⁵⁵³. Future studies examining whether these drugs exert their anti-angiogenic effects either directly via inhibition of the CXCL12/CXCR4 pathway, or indirectly through repression of the HIF transcription

factors, will provide valuable information regarding the mechanism of action of these drugs.

6.4 Perspectives and Concluding Remarks

Using primary patient specimens, *in vitro* tube formation assays and *in vivo* animal studies, the data presented in this thesis has shown that CXCL12 is an important mediator of MM-induced angiogenesis. Coupled with the knowledge that the CXCL12/CXCR4 axis is important in multiple disease processes in MM, these data suggest that inhibition of CXCL12 may be an effective strategy to target multiple aspects of MM biology. In addition, the conclusive data confirming the role of hypoxia and the HIF-1 and HIF-2 transcription factors in regulating aberrant CXCL12 and CXCR4 expression in MM PCs further adds to our current understanding of the CXCL12/CXCR4 axis in MM (Figure 6.2). These findings will hopefully aid the development of future therapeutic strategies directed at blocking the actions of CXCL12 in MM.

As a fitting conclusion to this thesis, it is important to reflect on the clinical significance of MM research. Myeloma patients are people facing terminal cancer, and are dependent on the latest research and breakthrough therapeutics to prolong their lives. While chemotherapy and stem cell transplantation have historically been the mainstay treatments for MM patients, the numerous side effects and physical toll of these approaches is sometimes too great for MM patients to withstand. In recent years, our understanding of MM biology has advanced significantly and this has led to the development of novel therapies which specifically target MM PCs and their microenvironment rather than blindly attacking cells at will. Drugs such as Thalidomide, Lenalidomide and Bortezomib have become powerful tools in the fight against MM, and have provided patients with increased quality of life and hope. With further research, targeted therapeutics will continue to improve patient outcomes, and perhaps one day MM will become a curable condition.

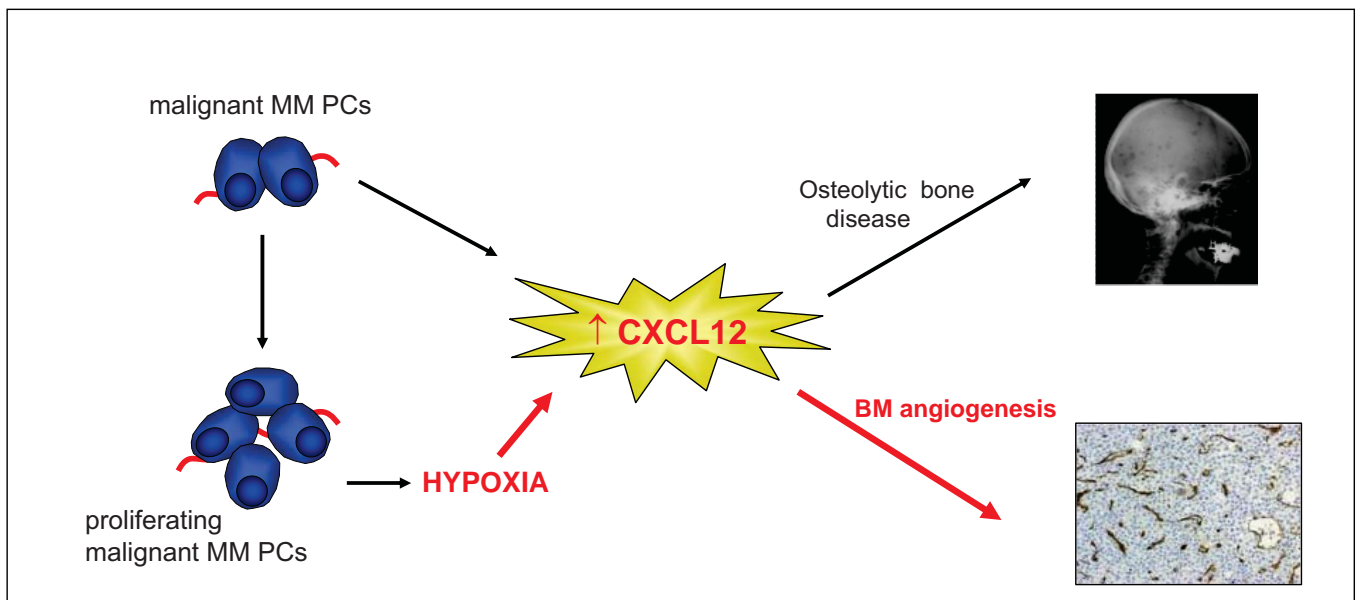


Figure 6.2. The Implications of Aberrant CXCL12 Expression in Myeloma Plasma Cells. Among the numerous phenotypic and genotypic changes associated with the malignant transformation to active MM is the increased expression of CXCL12. As demonstrated herein, hypoxia is an important mediator of aberrant CXCL12 expression in MM PCs. Elevated levels of CXCL12 in the blood circulation of MM patients correlate with the occurrence of osteolytic bone lesions and, as we now show, increased BM angiogenesis. Highlighted in red, the findings arising from this thesis provide important insights into the role of CXCL12 in MM.